THE EXPLOSION SEISMIC SOURCE FUNCTION: MODELS AND SCALING LAWS REVIEWED

Marvin D. Denny
Lawrence Livermore National Laboratory, Livermore, California 94550

Lane R. Johnson
Lawrence Berkeley Laboratory, Berkeley, Califlornia 94720

Abstract. The explosion seismic source function is the potential which satisfies the spherical P-wave equation. It is completely described by four properties. They are the steady-state value, roll-off, overshoot, and corner frequency. In one approach to describing the potential, the spectral roll-off is specified and the other properties are determined by fitting the data at prescribed times. In a variation of this approach, the roll-off is specified by assuming a radial stress of a known form is applied uniformly over a spherical surface, located at a range where the motion is assumed to be linear. In this review, it was found that of the four properties, less uncertainty exists about the steady-state value and the corner frequency than about the other two. A major problem has been scaling the results from one yield to another. New results are presented that show that, when the geophysical properties of the shot point are taken in account, cube-root scaling of the yield is appropriate for the steady-state value and the corner frequency, i.e., yield to the first and one-third powers, respectively. The new results also suggest that previous assumptions about the form of the applied radial stress are probably not appropriate. Finally, chemical and nuclear explosions appear in the new results to be indistinguishable, suggesting that experiments using chemical explosions could aid in reducing the remaining uncertainty in the seismic source function properties.

I. Introduction

In his review of seismic source models for underground nuclear explosions, Massé [1981] lists four unanswered questions and concludes from these that the seismic source for an underground nuclear explosion remains poorly defined after two decades of study. The third of Massé's questions, "What is the seismic source-time function for an underground nuclear explosion?" is the subject of this review. Rodean [1981] also found no consensus regarding the source function among seven papers that he reviewed and stated that there is disagreement about the far-field high-frequency displacement spectrum and about the overshoot in the source function. Therefore, as the fourth decade of underground nuclear testing begins, it is appropriate to re-visit some of this early work, to re-evaluate the conclusions of a decade ago, and to discuss some promising recent results that may lead to a consensus.

Explosion Source Phenomenology
Geophysical Monograph 65

This review begins with a discussion of the analytic models for the seismic source function of an underground explosion; considered are those with an instantaneous rise-time, with a finite rise-time, with no steady-state value, and with a steady-state value. Next, the proposed scaling laws are discussed. It concludes with a regression analysis of the relationships of the seismic moment and corner frequency parameters to the cavity size.

II. The Vibrating Sphere Problem: Assumptions and Definitions

In the vibrating sphere problem, an explosion is modelled at and beyond some critical distance where the material behaves elastically by a radial stress applied uniformly over a spherical surface. The spherical surface which separates inelastic from elastic response has been called the equivalent cavity by Sharpe [1942] and the equivalent radiator by O'Brien [1960], while the range to this surface has been called the elastic radius by Toksöz et al. [1964]. The solution of this problem is given below in terms of a potential which satisfies the P-wave equation. The description of the P-wave potential is the basic goal of the proposed explosion source models (Table 1). Two approaches have been taken to describe this P-wave potential. In one, the potential is described by approximating its time history with a parametric model evaluated at key times. In the other, the form of the radial stress is assumed to be known and its parameters are determined from key aspects of spectral data. While these approaches are equivalent, the second requires a more detailed physical knowledge. It is worthwhile, therefore, to begin with a review of the vibrating sphere problem.

The solution for this problem has been given by several authors: Jeffreys [1931, 1971, 1976]; Sharpe [1942]; Blake [1952]; Latter et al. [1959]; Cagniard (translated by Flinn and Dix [1962]); and Grant and West [1965]. Cagniard's derivation using Laplace transforms to simplify the notation will be followed here. In spherical coordinates the radial displacement and stress are given by

$$u_r = \frac{\partial \phi}{\partial r}, \tag{1}$$

and

$$\sigma_{rr} = \frac{(\lambda + 2\mu)}{\alpha^2}\frac{\partial^2 \phi}{\partial t^2} - \frac{4\mu}{r}\frac{\partial \phi}{\partial r}, \tag{2}$$

respectively, where λ and μ are the Lamé's constants, α is the compressional wave speed, and ϕ is the potential that satisfies the spherical wave equation

$$\nabla^2 \phi = \frac{1}{\alpha^2}\frac{\partial^2 \phi}{\partial t^2}. \tag{3}$$

The general solution of the wave equation for an expanding spherically symmetric disturbance is given by

TABLE 1. Proposed Source Models

Reference	Data	$s\bar{\psi}$	High-frequency asymptote	Initial motion	Final value	Radial stress
1. Toksoz, Ben-Menaham, and Harkrider [1964]	Regional Rayleigh waves	$-\frac{sRP_0}{\rho(s^2+2\eta\omega_e s+\omega_e^2)(s+\eta)^2}$	f^{-3}	$\dot{\mu}(0)=0$	0	$\sigma_{rr}=-P_0te^{-\varepsilon t}\mu(t)$
2. Haskell [1967]	Free-field	$\psi_\infty\frac{as+b^5}{(s+b)^5}$ (1)	f^{-4}	$\ddot{\mu}(0)=0$	ψ_∞	Not specified (4)
3. Mueller [1969]	Near-regional	$-\frac{sRP_0}{\rho(s^2+2\frac{\beta}{\alpha}\omega_e s+\omega_e^2)(s+\alpha)}$	f^{-2}	$\mu(0)=0$	0	$\sigma_{rr}=-P_0e^{-\alpha t}\mu(t)$
4. Mueller and Murphy [1971]; Murphy [1977]	Near-regional	$\frac{RP_p(s+\frac{P_0}{P_p}\omega_1)}{\rho(s^2+2\frac{\beta}{\alpha}\omega_e s+\omega_e^2)(s+\omega_1)}$	f^{-2}	$\mu(0)=0$	ψ_∞	$\sigma_{rr}=[(P_p-P_0)e^{-\omega_1 t}+P_0]\mu(t)$
5. von Seggern and Blandford [1972]	Teleseismic short-period *P*-wave	$\psi_\infty\frac{as+b^3}{(s+b)^3}$ (2)	f^{-2}	$\mu(0)=0$	ψ_∞	Not specified (4)
6. Helmberger and Harkrider [1972]	Long-period *P*- and Rayleigh waves	$\frac{s\psi_0\Gamma(\zeta+1)}{(s+\eta)^{\zeta+1}}$	$f^{-\zeta}$	depends on ζ	0	Not specified (4)
7. Helmberger and Hadley [1981]	Local *P*-wave	$\psi_\infty\frac{as+b^4}{(s+b)^4}$ (3)	f^{-3}	$\dot{\mu}(0)=0$	ψ_∞	Not specified (4)
8. Denny and Goodman [1990]	Free-field and local	$\psi_\infty\frac{\omega_c^2\omega_1}{(s^2+2\eta\omega_c s+\omega_c^2)(s+\omega_1)}$	f^{-3}	$\dot{\mu}(0)=0$	ψ_∞	Not specified (4)

(1) a = (24 B + 1)k^4 and b = k in Haskell's notation.
(2) a = (1 – 2 B)k^2 and b = k in von Seggern and Blandford notation.
(3) a = (6B + 1)k^3 and b = k in Helmberger and Hadley notation.
(4) Not specified by reference but may be derived from equation (6).

$$\phi(r,t)=-\frac{1}{r}\psi(\tau), \tag{4}$$

where ψ is determined once the radial stress, σ_{rr}, at $r=R$ is specified and τ is the reduced time, $\tau=t-(r-R)/\alpha$, . According to Rodean [1981], the function ψ was first called the *reduced displacement potential* or RDP by Werth et al. [1961] because it is dependent on just the reduced time variable. Substituting (4) into (2), and taking the Laplace transform with respect to τ, the radial stress is then given by

$$\bar{\sigma}_{rr}=-\frac{\rho}{r}\bar{\psi}(s^2+\frac{4\beta^2}{\alpha r}s+\frac{4\beta^2}{r^2}), \tag{5}$$

where ρ is the density and β is the shear wave velocity. With $\bar{\sigma}_{rr}$ specified at some range R, the RDP is from (5)

$$\bar{\psi}=\left.\frac{-r\bar{\sigma}_{rr}}{\rho(s^2+2\eta\omega_e s+\omega_e^2)}\right|_{r=R}, \tag{6}$$

where the bar denotes the Laplace transformation, $\eta=\beta/\alpha$, $\omega_e=2\beta/r$, and R is greater than or equal to the elastic radius.

For a step in pressure, $p(t)=P_0U(t)$ where P_0 is the amplitude of the pressure applied to the inside of a spherical surface at $r=R$ and $U(t)$ is the Heaviside step function, i.e. $U(t)=1$ for $t\geq 0$ and $U(t)=0$ otherwise, the radial stress is given by

$$\bar{\sigma}_{rr}=-P_0/s. \tag{7}$$

In this case, (6) becomes

$$\bar{\psi}=\frac{P_0R^3\omega_e^2}{4\mu s(s^2+2\eta\omega_e s+\omega_e{}^2)}, \tag{8}$$

where $\omega_e=2\beta/R$. The initial- and steady-state values, ψ_0 and ψ_∞ respectively, of the inverse of (8) can be readily evaluated from the initial- and final-values theorems, Cheng [1959]. The final-value theorem states that $lim\{f\}_{t\to\infty}=lim\{s\bar{f}\}_{s\to 0}$ and the initial-value theorem states that $lim\{f\}_{t\to 0}=lim\{sf\}_{s\to\infty}$, where f is an arbitrary function. Thus, ψ_0 and ψ_∞ are 0 and $P_0R^3/4\mu$, respectively. The inverse solution to (8) can be found in any table of Laplace transforms, e.g., Bateman [1954], and is

$$\psi = \frac{P_0 R^3}{4\mu}(1 - \frac{\omega_e}{b}e^{-a\tau}sin(b\tau + \theta)), \quad (9)$$

where $a = \eta\omega_e$, $b = \omega_e\sqrt{1-\eta^2}$, and $\theta = tan^{-1}(b/a)$ and the initial- and steady-state values are as expected. Rodean [1971] illustrates the results for this and three other cases of radial stress.

Equations (8) and (9) are well known in the engineering fields. In mechanical engineering, they describe a simple mass suspended on a spring: ω_e is the undamped circular frequency ($2\pi f$) of oscillation, b is the damped circular frequency, and η is the damping factor. Gurvich [1965] described (6), (8) and (9) in terms of a resonance filter. In fact in electrical engineering, they describe a low-pass filter whose *order* is determined by the number of the roots of the numerator or denominator of the rational polynomial (8), whichever is larger. The *poles* are the roots of the denominator and the *zeroes* are the roots of the numerator. In general, the RDP (6) is the result of applying a second-order low-pass filter to the radial stress. Thus, the order of (6) is the number of poles of the radial stress plus two. In the case of a step in radial stress (8), for example, the RDP is a third-order low-pass filter with 3 poles and no zeroes.

In the seismic source problem, the damping factor in terms of Poisson's ratio, ν, is

$$\eta = \sqrt{\frac{1-2\nu}{2(1-\nu)}}. \quad (10)$$

As Poisson's ratio ranges between zero and one half, η ranges between $\sqrt{2}/2$ and zero. This range of damping means that (9), beginning at zero, rises to a peak at $\tau = \pi/b$ and then dies out to a steady state value of ψ_∞. In other words, it overshoots the final value and then oscillates with decreasing amplitude about it. The amount of *overshoot*, i.e. the ratio of the peak to the final value, is determined by the damping and increases as η decreases. In mechanical engineering, this response is described as under-damped and, in electrical engineering terms, as a good-to-poor oscillator depending on the damping.

The derivative of ψ is called the *reduced velocity potential* (RVP) and is a more convenient function to work with than is the RDP. This is due to the properties of its spectrum and to the fact that it is proportional to the far-field displacement. These features are discussed below. In spite of these more convenient features of the RVP, the RDP is commonly called the *seismic source function*.

For an RDP with a non-zero final value such as (8), the modulus of the spectrum of the transformed RDP ($|\bar{\psi}|_{s=i2\pi f}$) is infinite at $f = 0$ but that of the transformed RVP ($|s\bar{\psi}|_{s=i2\pi f}$) is finite at $f = 0$ and is equal to ψ_∞. The modulus of the transformed RVP is, therefore, commonly plotted instead of that of the RDP. From such a plot four basic source function characteristics (*seismic moment, corner frequency, overshoot,* and *roll-off*) can, in principle, be estimated. The seismic moment for explosions, introduced by Müller [1973] and Aki et al. [1974], is

$$M_0 = 4\pi\rho\alpha^2\psi_\infty. \quad (11)$$

The corner frequency, f_c, is the frequency where the transformed RVP's low-frequency asymptote intersects its high-frequency asymptote. From (6), it can be seen that the RDP always has a corner frequency, even in the simple case of an impulse in radial stress. The roll-off is the exponent of the high frequency asymptote ($f \to \infty$) of the transformed RVP or, equivalently, of the far-field displacement spectrum. The roll-off is equal to the difference between the number of zeroes and the number of poles. In (8), the corner frequency is the same as the *boundary condition eigenfrequency*, i.e. the magnitude of the complex pair of poles specified by the boundary condition divided by 2π, $f_e = \omega_e/2\pi$. The roll-off, in this case, is -2.

It should be noted that the boundary condition eigenfrequency is, in general, not the same as the corner frequency. For example, Denny and Goodman [1990] have shown that for the nuclear explosion SALMON, $(f_e)_{r=R_e} < f_c$, where R_e is the elastic radius. In this case, the corner frequency was determined by the radial stress.

The fact that the displacement is proportional to the RVP at sufficiently large ranges (called the *far-field*) is readily shown as follows. From (1) and (4), the transformed radial displacement, $\bar{u}_r$, is given by

$$\bar{u}_r = \frac{\bar{\psi}}{\alpha r}(s + \frac{\alpha}{r}). \quad (12)$$

The contribution of the term, $(s + \frac{\alpha}{r})$, in (12) is important only for ranges (called the *near-field*) where r is not much greater than α/ω_c, where $\omega_c = 2\pi f_c$. As the range increases, α/r becomes negligible compared to ω_c and $s + \alpha/r \simeq s$ so that the far-field transformed displacement, $\bar{u}_{ff}$, becomes

$$\bar{u}_{ff} \simeq \frac{s\bar{\psi}}{\alpha r}. \quad (13)$$

Thus, the spectrum of the far-field displacement is proportional to the transform of the derivative of the source function.

Finally, the far-field transformed kinetic energy radiated per unit surface area by the vibrating sphere, $\bar{E}_A$, is [Aki and Richards, 1980, page 127]

$$s\bar{E}_A = \frac{1}{2}\rho\alpha\bar{v}^2, \quad (14)$$

where $\bar{v}$ is the transformed particle velocity. The total energy radiated, E_T, is then, by Parseval's theorem

$$E_T = \frac{\rho\alpha}{2\pi}\int_{-\infty}^{\infty}\bar{v}(i\omega)\bar{v}(i\omega)^* df, \quad (15)$$

where the asterisk denotes the complex conjugate. For a step function in radial stress (15) becomes with the use of (13), (8), and (11)

$$E_T = \frac{\pi^2 f_c^3 M_0^2}{2\eta\rho\alpha^5}. \quad (16)$$

It can also be shown, in other cases where the transformed RVP's roll-off is steeper than -2, that the energy is still proportional to $f_c^3 M_0^2$.

III. The RDP: Review of Experimental Results

There has never been a clear relationship established between source functions determined from the *close-in* (< 10 km) data and the source function for teleseismic data. The concern has been that the teleseismic observations depend on the medium properties below the source volume and within perhaps several wavelengths of the *working point* (i.e., the detonation point), while the close-in observations sometimes only sample a very narrow aperture above or to one side of the working point and within a range comparable to perhaps one teleseismic wavelength. Efforts to establish such a relationship will be reviewed in this section. Three of the four source function characteristics identified above will be reviewed in this section; the fourth (corner frequency) will be addressed in the next section. The question of the steady-state value of the source function will be dealt with first, followed by the roll-off and the overshoot. Of the three, the steady-state issue seems to be the best and the overshoot the least well understood.

A. Steady-State Value

As pointed out above, (6) shows that the source function is a low-pass version of the applied radial stress. Therefore, if the radial

stress has a steady-state value, the source function also has one. In the following the observations recorded in the literature are summarized. Some authors refer to radial stress while others write of the source function.

Brune and Pomeroy [1963] were the first to infer the character of the explosion source function from *regional* seismic data (100 to 1000 km). They studied the radiation patterns and the phase spectra of Rayleigh waves. Explosions in alluvium and tuff were found to have a characteristic explosion radiation pattern and to be consistent with the phase of a step in radial stress. Unfortunately, a different conclusion was reached by Toksöz et al. [1964] who analyzed long-period Rayleigh wave data also taken at regional distances. After removing from the data the contribution of the path and recording instrumentation, Toksöz et al. concluded that a radial stress of the form $\sigma_{rr} = -P_0 t e^{-\xi t} U(t)$, where ξ is an arbitrary parameter, fit the data better than did a step function. Thus, a controversy began.

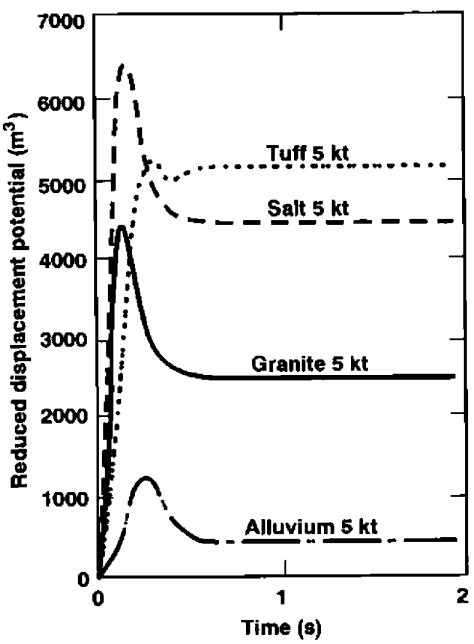

Fig. 1. Reduced displacement potentials. The data in this figure are from Werth and Herbst [1963], Fig. 2. All have an overshoot except tuff. Murphy [1979] shows the results from another gage, where a surface reflection was not a problem, on the same experiment (RAINIER) with a significant overshoot.

The first experimental data, in the form of RDP's, were reported by Werth and Herbst [1963]. The data, reproduced in Figure 1, were taken in the *free-field* from nuclear explosions in tuff (RAINIER), alluvium (FISHER), granite (HARDHAT), and salt (GNOME). To be in the free-field, the gages must be buried in the medium deep enough so that the compressional wave is recorded without interference of surface reflections. As shown in Figure 1, all four RDP's rise to a maximum (overshoot) and then decay to a steady-state value. Berg and Papageorge [1964] fit the RDP at 398 m on GNOME with a step in radial stress, obtaining only a fair fit to the data. Haskell [1967] proposed a general model (Table 1) to describe the overshoot and steady-state value of all four RDP's. Unfortunately, the duration of the free-field data is short as seen in Figure 1 and noise in the signal makes computation of the steady-state value difficult and introduces uncertainty in the result. For this reason and the source volume sampling problem described above, the relationship of free-field estimates of the source function's steady-state component to teleseismic and surface-wave signals became a cause for concern.

Liebermann and Pomeroy [1969] and Molnar et al. [1969], studying the M_s/m_b discriminant, concluded that a plausible explanation for the discriminant's success is that the source function for an earthquake has a steady-state value while that for an explosion does not, implying that the radial stress for an explosion is a decaying pulse of the form given by Toksöz et al. [1964]. Savino et al. [1971], studying Rayleigh waves from earthquakes and explosions from the Western US, the Aleutians, Novaya Zemlya, and Central Asia, came to the same conclusion. Mueller [1969] modelled the spectra of seismic data taken at *near-regional* distances (<200 km) from several explosions at the Nevada Test Site (NTS) using a simple exponentially decaying radial stress model with seemingly satisfactory results. After studying both short- and long-period data, Helmberger and Harkrider [1972] found that the Haskell model was adequate for short-period data but not for predicting the long-period observations. To overcome this deficiency, they proposed a model (Table 1) with no steady-state component. Thus, until 1972, many investigators clearly favored no steady-state value.

Others were unsure about the nature of the long-period behavior of the source function. Molnar [1971], though finding the spectra for teleseismic P-waves from the explosions JORUM and HANDLEY to decrease rapidly with period ($\propto T^{-2}$) in the range of 1 to 20 sec, concluded that this could be due either to the modulating effect of the surface reflection, pP, or to the explosion source function. He also found that the data were not of sufficient quality or quantity to rule out any linear combination of impulse and step function components in the source function, unless other data demonstrate that the surface reflection does not have a major effect on the observed spectrum. If this were true, he concluded the data would then prove that the source function is primarily an impulse. Wyss et al. [1971] undertook a study similar to that of Molnar using teleseismic P-wave data from the Amchitka explosions, MILROW and LONGSHOT, and four shallow earthquakes in the Aleutian Islands and came, essentially, to the same conclusions. Müller [1973], introducing the idea of the seismic moment for explosions, found that strain measurements made on the explosion BENHAM at local distances (28-29 km) were consistent with a step function, but he was puzzled by the apparent long-period P-wave explosion spectra behavior that appears to be consistent with an impulsive source noted by other investigators.

While the case against a steady-state value became increasingly clouded, the argument for a steady-state value slowly became more convincing. Haskell [1961] solved the quasi-static problem of an expanding cavity in a plastic medium. This solution showed that the far-field permanent displacement and, hence, the steady-state value of the source function are dependent on the final cavity size. Von Seggern and Lambert [1970], studying spectral ratios of Rayleigh waves of both earthquakes and explosions between periods of 10 and 50 sec, found them to be consistent with Haskell's model. Tsai and Aki [1971] studied the Rayleigh waves from 10 small and 3 large underground explosions at NTS recorded at *far-regional* distances (940 and 2405 km). They found the results to be in excellent agreement with Haskell's model. Mueller and Murphy [1971] used the quasi-static idea of computing the final displacement and, hence, the RDP under the assumption of incompressibility from the cavity size in their proposed source model (Table 1). Aki et al. [1974] also endorsed this line of reasoning and argued that a nuclear explosion must have a steady-state value. They also considered a spherical shell surrounding the non-elastic zone of an explosion, explaining that this shell stretches during the passage of the shock waves and remains stretched because part of the strain is plastic. The source function for explosions must then be a step function for long periods since

the relaxation time for plastic deformation is much longer than the seismic periods; indeed, since explosions create permanent cavities, it is infinite. Burdick and Helmberger [1979], in modelling teleseismic short- and long-period body waves, chose not to use the model of Toksöz et al. [1964], Mueller [1969], or Helmberger and Harkrider [1972] since these models do not have a step component and, in their words, "Some dc component should realistically be expected if a cavity is formed by the explosion." As seen in Table 1, this argument apparently was powerful enough for two investigators to change their opinion; see Mueller [1969], Mueller and Murphy [1971], Helmberger and Harkrider [1972], and Helmberger and Hadley [1981]. And, finally, Patton [1982] applied the method of Brune et al. [1960] to 4 NTS explosions and showed clearly that the spectral phases of the Rayleigh waves are consistent with a step function.

Having given a very persuasive argument for a steady-state value, Aki et al. [1974] then argued that the seismic moment as estimated from free-field data is high by a factor of 3 as shown in Figure 2a, the underlying assumption being that the seismic moment should be independent of the source media. However, this assumption is not necessarily true and the apparent discrepancy may not be as bad as Figure 2a shows. Murphy [1974] explained some of the variance as being due to differences in the source properties. Assuming that the higher yield explosions are generally at Pahute Mesa while the lower yield ones are at Yucca Valley, he derived a moment-magnitude relationship, Figure 2b, for each region based on typical P-wave sound speeds and densities, using the incompressibility relationship

$$\psi_\infty = R_c^3/3, \tag{17}$$

where R_c is the cavity radius. In addition, Denny and Goodman [1990] have shown that the SALMON moment (the larger magnitude of the two salt data points) should be lower by 40%, bringing it reasonably close to the surface wave line in Figure 2a. The SALMON datum was over-estimated because the estimate was made from data taken in the non-linear zone which is easily identified by a peak particle velocity spatial rate of decay exceeding that expected from (13) for linear motion, i.e., r^{-1}. As shown by Denny and Goodman, estimates made in this region are too large due to large permanent displacements associated with plastic yielding. This is probably the case for the other explosions in hard-rock (e.g. granite, salt, dolomite, shale, etc.) as well. This same conclusion was also reached by Bache [1982]. Furthermore, Werth and Herbst [1963] do not provide any evidence that the measurements for the four explosions they reported are in the linear region. A cursory perusal of the peak particle velocity data given by Perret and Bass [1975] suggests, that of the explosions in Aki's table, the measurements for GNOME, HARDHAT, HANDCAR, and GASBUGGY were probably in the non-linear zone, while the RAINIER and FISHER measurements may have been in the linear zone.

From the foregoing it seems possible that differences between close-in and regional surface wave observations can be resolved. Another indication that this might be true is given by Murphy (this volume; see Figure 5.) In Murphy's Figure 5, the ratio of the regional surface wave moments of Aki et al. [1974] to the moment computed from (17) is shown. The explosions in Yucca Valley seem to be more consistent than those at Pahute Mesa. As suggested by Patton (this volume), this apparent discrepancy may be due to a systematic difference in the release of tectonic energy by the higher yield explosions, typically located at Pahute Mesa.

B. Roll-off

The asymptotic behavior of the RVP at high frequencies depends on the form of the radial stress. From (6), it can be seen that the roll-off will be steeper than -2 if the transform of the derivative of the radial stress has more poles than zeroes.

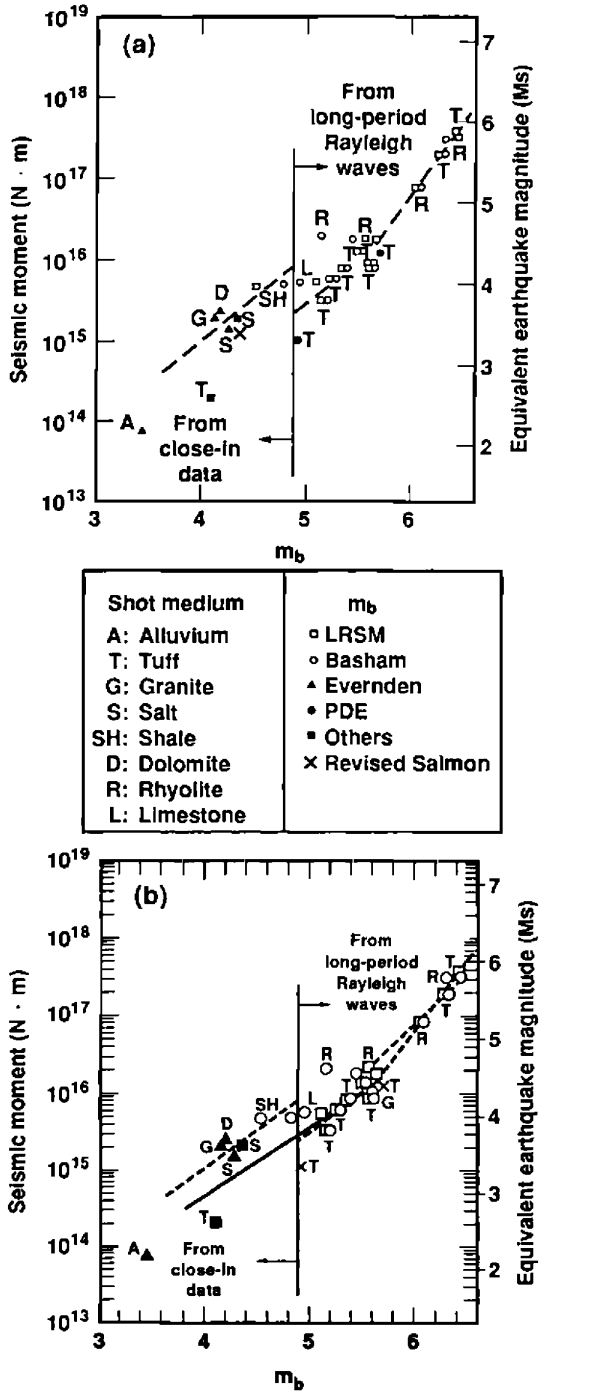

Fig. 2. Seismic moments vs magnitude. (a) This is Fig. 1 of Aki et al. The moments on the left-hand side were computed from free-field data while those on the right-hand side were computed from long-period surface wave data. Based on this figure Aki et al. thought that the free-field data were high by a factor of 3. (b) This is Fig. 1 of Murphy [1974]. Some of the variance can be accounted for by differences in the source media. The upper line is for Pahute Mesa and the lower one is for Yucca Flats. Some of the discrepancy is probably also due to data taken in the inelastic region. Such estimates from these data are expected to be high.

In the relatively simple case of a step function radial stress, the order of the model given by (8) is 2 and the roll-off is -2 since it has no zeroes. More complicated radial stresses, requiring higher order models, can also have a roll-off of -2. Models 3 and 4 in Table 1 are examples of third order models with -2 roll-offs. In model 3, Mueller [1969] assumed an exponentially decaying radial stress,

$$\sigma_{rr} = -P_0 e^{-\alpha\tau} U(\tau), \tag{18}$$

while in model 4, Mueller and Murphy [1971] assumed that the radial stress is a combination of a Heaviside step function and an exponentially decaying term,

$$\sigma_{rr} = -(P_0 + P_1 e^{-\omega_1 \tau}) U(\tau). \tag{19}$$

The transformed derivatives of the radial stresses of (18) and of (19) are

$$s\bar{\sigma}_{rr} = -P_0 \frac{s}{s+\alpha}, \tag{20}$$

and

$$s\bar{\sigma}_{rr} = -P_0 \frac{(1 + P_1/P_0)s + \omega_1}{s+\omega_1}, \tag{21}$$

respectively. Both (20) and (21) have one pole and one zero. Therefore, even though the order for both RVP's is three, the roll-off is -2. This is true since the high-frequency asymptotes of the moduli of (20) and (21) are constants, P_0 and $P_0 + P_1$, respectively.

Haskell's model (2, Table 1) is an example of a model where the implied radial stress has more poles than zeroes. This model was derived by requiring acceleration to be continuous at $\tau = 0$. Application of (13) and the initial-value theorem to this model shows that it is, in fact, continuous to acceleration and that its roll-off is -4. Similarly, models with roll-offs of -3 and -2 are continuous at $\tau = 0$ to velocity and displacement, respectively.

Von Seggern and Blandford [1972] noted that Haskell's model, when scaled up in yield, failed to satisfy the spectral ratios of short-period teleseismic data from the three nuclear explosions at Amchitka. They were able to obtain a better fit of the spectral ratios using model 5 (Table 1) with a roll-off of -2. This model was obtained by reducing the order of Haskell's model by two.

Peppin [1976] computed 140 P-wave spectra of explosions, earthquakes, and explosion-induced aftershocks, all within the NTS and all from wide-band seismic data at local (<30 km) and near-regional distances (200 to 300 km). From these he concluded that the far-field source spectra decay at least as fast as frequency cubed; a roll-off of -3 or steeper.

Helmberger and Hadley [1981) showed that a model continuous only to displacement produces an unrealistic discontinuity in synthetic seismograms and, therefore, is unsatisfactory. Their model (7, Table 1) is continuous to particle velocity and was obtained by reducing the order of Haskell's by one, for a roll-off of -3. Using this model, Lay et al. [1984] satisfactorily modelled the teleseismic data from the Amchitka nuclear explosions. The model's roll-off of -3 did not cause any problems in the 0.5- to 3-Hz range as found by von Seggern and Blandford [1972] with Haskell's original model. The difference was not in the change of the roll-off, but in the fact that Lay et al. used the empirically obtained corner frequencies of Helmberger and Hadley [1981]; whereas, von Seggern and Blandford simply cube-root scaled those obtained by Haskell for granite.

Denny and Goodman [1990], borrowing electrical engineering system identification techniques, modelled the free-field data and the spectral ratios of *local* (10 to 111 km) seismic data from the nuclear explosions, SALMON and STERLING, in salt with a rational polynomial. They found that a third-order model (Table 1) was required to adequately describe the rise-time observed in the free-field data and the high-frequency roll-off of -3 observed in the spectral ratios of the two explosions.

Of the models of Table 1, four of the six earliest ones (1, 3, 4, and 6) were obtained by specifying the radial stress. The others were determined by approximating the shape of either the reduced displacement potential (models 2, 5, and 7) or the reduced acceleration potential (model 8). The radial stress implied by these models can be determined from (5) for any specified range. The range of most interest, of course, is the one where the motion first becomes linear; thus, equating (6) to model 8 (Table 1), the radial stress for SALMON at the elastic radius can be estimated by

$$\bar{\sigma}_{rr} = \psi_\infty \frac{\rho(s^2 + 2\eta_e\omega_e s + \omega_e^2)\omega_c^2\omega_1}{R_e(s^2 + 2\eta_c\omega_c s + \omega_c^2)(s+\omega_1)}, \tag{22}$$

where ψ_∞ = 2200 m^3, η_e = 0.55, η_c = 0.6, ρ = 2200 kg/m^3, and ω_c, ω_1, and ω_e are 36.4, 29.4 6.3 rad/sec, respectively, as determined by Denny and Goodman [1990]. To estimate the elastic radius some independent information must be used. For the SALMON explosion, Denny and Goodman estimated the location of the elastic radius by extrapolating the peak particle velocity data for both the SALMON and the STERLING explosions to the range where the linearity threshold is crossed. In this case, threshold is based on the amplitude of the *elastic precursor*. (The elastic precursor is thought, Glenn [1990], to be the result of strain hardening and it propagates, in this case, in the inelastic region with an amplitude equal to the threshold value of about 0.3 m/s and at P-wave speed, ahead of a larger, slower plastic wave. The elastic precursor and the plastic wave ultimately become a single wave travelling at P-wave speed when the particle velocity falls below the threshold.) Using this procedure, an elastic radius of about 800 m was found. The corresponding radial stress computed from (22) is as shown in Figure 3 and looks like a damped sine-wave superimposed on a small step function.

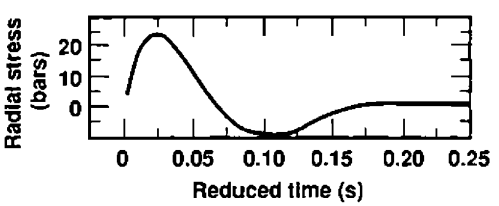

Fig. 3. Radial stress. This is Fig. 22 from Denny and Goodman [1990] showing the estimated radial stress at the elastic radius for SALMON. Note that the final steady state value of about 2 bars occurs outside the time frame shown and from (6) the RDP is a low-pass version (f_c~1Hz) of this signal.

An interesting, worthwhile exercise would be to derive the equivalent radial stress for those few explosions where free-field radial particle velocity measurements were made at several ranges. For those explosions whose data are only in the non-linear zone, the results would obviously be fictitious but their progressive change in shape with range should be enlightening.

C. Overshoot

The free-field data of Werth and Herbst [1963], Figure 1, show a significant overshoot for both hard-rocks, granite and salt; however, for the porous rocks the data show a significant overshoot for alluvium but not for tuff. Subsequent studies have produced contradictory results with the only point of agreement being the result for alluvium. The alluvium data of Werth and Herbst is consistent with that of Perret [1971] for the MERLIN explosion and of Murphy and Bennett [1979] for the FISHER and the MERLIN explosions. Murphy and Bennett also studied free-field data for the explosions RAINIER, MUDPACK, and DISCUS THROWER in tuff.

The DISCUS THROWER data were taken close to the tuff/paleozoic interface making the signals too complex to use. For RAINIER, they found, for a gage most likely in the linear zone and also less likely to be affected by a surface reflection than the one used by Werth and Herbst, an overshoot of about 2 to 1. MUDPACK also showed a significant overshoot. Finally, Denny and Goodman [1990] studying SALMON found no significant overshoot for salt. Therefore, if the salt and granite data, given by Werth and Herbst, are in error and this is a strong possibility because the data in question were taken in the non-linear region, then one might conclude that porous media have a significant overshoot while non-porous media do not. The conclusion for the porous media seems well established but the one for hard-rock is more speculative.

Other contradictory observations have been made. Aki et al. [1974] compared local data taken at NTS with long-period Rayleigh wave data and concluded that a large overshoot in the source function, 4 or 5 times the residual value, is required to explain both sets of data. Peppin [1976] concluded from his study of 140 explosions and earthquakes that source spectra of explosions in tuff are flat from 0.2 to 1.0 Hz (no overshoot).

Burdick and Helmberger [1979] modelled teleseismic short- and long-period body waves using synthetic seismograms and concluded that the source function must have a substantial overshoot. Helmberger and Hadley [1981] tried to deduce the overshoot parameter (controlled by the zero in the RDP) in their model from close-in data recorded at 8 km on JORUM. The frequency parameter (k in ref. 7, Table 1) was readily determined by the dominant period of the data, but the overshoot parameter, B, could not be uniquely determined for two reasons. First, the arrival times of pP and/or related slapdown phenomena are such that they arrive during the later half of the direct P-wave and are superimposed on it; and second, the bandwidth of the data is such that the zero in the Helmberger-Hadley model makes an important contribution and cannot be separated from ψ_∞.

Douglas and Hudson [1983] demonstrated that the main features of the WWSSN seismograms shown by Burdick and Helmberger [1979] and Helmberger and Hadley [1981] can be accounted for with a source with no significant overshoot. Reverberations in the crust at the source and the receiver can account for most of the variations in the observed Novaya Zemlya WWSSN LP seismograms shown by Burdick and Helmberger [1979], making it impossible to draw any firm conclusions about the overshoot. Burdick et al. [1984] did essentially the same analysis as Helmberger and Hadley [1981] but on the Amchitka explosions, MILROW and CANNIKIN, using local data (recorded at 7 to 20 km). The Helmberger-Hadley [1981] model parameters were evaluated for both explosions. They found, as others had, that the overshoot parameter could not be resolved.

In the Mueller-Murphy model the zero is yield dependent, making the overshoot also dependent on yield. In the previous section, the low- and high-frequency asymptotes for this model were shown to be P_0 and $P_0 + P_1$, respectively. The ratio of high- to the low-frequency asymptote controls the overshoot; the higher the ratio, the larger the overshoot. In the Mueller-Murphy model this ratio is a proportional to $h^{0.07}W^{0.13}$ where h is the depth of burial and W is the yield. This feature is contrary to that found by Lay et al. [1984] who determined that the Helmberger-Hadley [1981] source model is best fit if the amount of overshoot decreases with increasing yield or depth of burial.

These contradictory results open the field for other interpretations. One possibility is that the overshoot is controlled by neither the depth nor the yield. Depth of burial in all these models could be just a surrogate variable for some working point material property. Then the overshoot could be independent of yield and depth and dependent only on the working point's material properties. Also, the effect of spall could mimic overshoot in far-field spectral observations (c.f. Taylor and Randall [1989]).

IV. Scaling: Theory and Observations

A. *Theory*

Cube-root scaling comes from a simple energy, volume relationship. For a given chemical explosive, its *specific energy*, i.e., energy per unit mass of an explosion, is a constant so that its energy release is simply dependent on the mass, or volume, of the explosive. For a nuclear explosion, the volume of the fireball in air or of the vaporized zone in the earth is proportional to the energy. The energy released by a nuclear explosion is called its yield and is given in *kilotons* ($1\ \mathrm{kt} = 4.2 \times 10^{12}\mathrm{J}$) while the energy or yield of a chemical explosion is usually quoted in *kilograms* even though all chemical explosions do not have the same specific energy. Since the units of volume are length cubed, the yield is proportional to length cubed, or conversely, length (l) is proportional to the cube-root of the yield ($l \propto W^{1/3}$). Specific energy has the units of length divided by time, all squared ($(l/t)^2$). Therefore, in order for the units of the specific energy to be consistent, time must also be proportional to the cube-root of the yield ($t \propto W^{1/3}$), where time refers to fireball or cavity growth. From (8), the RDP is seen to have the units of volume while those of the seismic moment are the same as energy. Therefore, both quantities should *scale as* (i.e., be proportional to) the yield to the first power. Frequency, obviously, should be inversely proportional to the cube-root of the yield.

Care must be taken when scaling data. Amplitudes from narrow- and wide-band data do not scale in the same ways and time can not be scaled when recorded on narrow-band systems. Only time in the source function can be scaled. Arrival times obviously can not be scaled. Therefore, only reduced time from signals recorded by wide-band instrumentation, i.e., bandwidth greater than the corner frequency of the signal, and in the free-field can be scaled.

Insight into how ground motion scales with yield can be gained from the problem of the vibrating sphere. For a step in applied pressure, the far-field transformed displacement is obtained by substituting (8) into (13),

$$\bar{u}_{ff} = \frac{\psi_\infty \omega_e^2}{\alpha r(s^2 + 2\eta\omega_e s + \omega_e{}^2)}. \tag{23}$$

At a fixed range, the only quantities in (23) that scale are ψ_∞ and ω_e. Therefore, for low frequencies ($f < \omega_e/2\pi$), the ground motion in all of its forms (displacement, velocity, and acceleration) is then proportional to ψ_∞ while for high frequencies ($f > \omega_e/2\pi$) they are proportional to $\psi_\infty \omega_e^2$. Thus, for low frequencies the ground motion scales as the first-power of the yield while for high frequencies, it scales as the cube-root of the yield. This result has been derived by several investigators, e.g., O'Brien [1957,1960], Latter et al. [1959], and Carpenter et al. [1962].

Broadband displacements and velocities, however, do not scale in the same way. From (9) and (13), the broadband far-field displacement is

$$u = \frac{\psi_\infty \omega_e}{\alpha r(1-\eta^2)^{1/2}} e^{-a\tau} sin(b\tau), \tag{24}$$

and the velocity is

$$v = \frac{\psi_\infty \omega_e^2}{\alpha r(1-\eta^2)^{1/2}} e^{-a\tau} cos(b\tau + \theta), \tag{25}$$

where $\theta = tan^{-1}(a/b)$. From (24) and (25), it can be seen that at a fixed range displacements would be expected to scale as the two-thirds power of yield and velocities as the one-third power of yield.

This may seem like a contradiction, since the units of particle velocity and displacement would indicate that the former should be independent of yield and the latter should be proportional to the cube-root of the yield. When viewed in terms of the *scaled range*, $R/W^{1/3}$, however, there is no contradiction. Particle velocity is then seen to be independent of yield and displacement is seen to be proportional to yield to the one-third power while both are inversely proportional to the scaled range. Free-field data are typically presented in this form, e.g., Perret and Bass [1975].

Carpenter et al. [1962] used cube-root scaling of free-field data from the RAINIER explosion to study the amplitude-yield scaling question. They concluded that for most practical applications (meaning narrowband recordings) it appears that a power law can be used, although for very large charges (or high frequencies) the amplitude will increase less rapidly than charge size and may even decrease. This effect is due to the bandwidth of the recording instrument. For small explosions the corner frequency would be above the frequency of the peak response of the seismograph, but for larger ones the corner would move closer until finally it would be below the peak response. Similar results were obtained by Werth and Herbst [1963] and by Berg and Papageorge [1964]. Thus, the amplitude measured on a narrowband seismograph could be expected to be $A \propto W^b$, where b ranges from 1.0 to 1/3. Since the seismic magnitude is proportional to the log of the amplitude, $m \propto \log A$, then the seismic magnitude is proportional to the log of the yield, $m \propto b \log W$. If the corner frequency of the signals are always greater than the frequency of the peak response of the seismograph, as it is for the long-period WWSSN seismograph, then the slope or exponent b would be expected to be unity.

Mueller [1969] assumed that the medium "on the large" has low tensile strength and that the limiting pressure is therefore in the neighborhood of the overburden pressure in order to keep the medium from going into tension and propagating cracks. Mueller and Murphy [1971, Table 1] used this logic to infer from analysis of near-regional and free-field data that the peak pressure, P_p, is 1.5 times overburden, i.e., $P_p = P_0 + P_1 = 1.5\rho g h$, where P_0 and P_1 are the same as in (19), h is the depth of burial and g is gravity. They also assumed that the peak pressure follows a power law in the inelastic region, $P_p \propto (r/W^{1/3})^{-n}$. Equating these two relationships for the peak pressure, they determined the elastic radius to be related to overburden as follows

$$\frac{R_e}{W^{1/3}} \propto \frac{1}{(\rho g h)^{1/n}}. \tag{26}$$

Invoking the incompressibility argument, they found

$$P_0 = \frac{4\mu}{3}\left(\frac{R_c}{R_e}\right)^3, \tag{27}$$

where the cavity radius, R_c, from empirical studies is given by $R_c = cW^{0.29}h^{-0.11}$. At low frequencies the Mueller-Murphy model predicts that ψ_∞ and, therefore, amplitudes should scale as $W^{0.87}/h^{0.33}$, while at high frequencies they scale as $W^{1/3}h^{0.583}$. Assuming that the depth of burial scales as the cube-root of the yield, these scaling laws become $W^{0.76}$ and $W^{0.527}$, respectively.

It is worth noting that ground motion scaling at high frequencies ($f > f_c$) proportional to the cube-root of the yield applies only to a model whose roll-off is -2. When applying cube-root scaling to a model whose roll-off is -3, the spectral amplitudes at high frequencies are found to be independent of yield; while for a model whose roll-off is -4 such as Haskell's, they decrease with yield. For a model with a roll-off of -3 or -4 to have high-frequency amplitudes increasing with yield the corner frequency must somehow be modified either through some inherent depth dependence or through some material property which changes uniformly with depth so that the corner frequency would ultimately depend inversely on yield to some power less than 1/3 or 1/4, respectively.

Yield is not the only important property that determines the corner frequency. If the energy deposited by an explosion into the surrounding material is a given fraction of the yield for a given material then, by (16)

$$f_c^3 \propto \rho\alpha^5 E/M_0^2. \tag{28}$$

As discussed above, Mueller and Murphy [1971] hypothesized that the elastic radius, which by their definitions is proportional to α/f_c, is inversely dependent on the overburden as in (26). Thus, the corner frequency would be expected to be directly dependent on the overburden and inversely dependent on the cube-root of the yield

$$f_c^3 \propto \alpha^3(\rho g h)^{3/n}/W. \tag{29}$$

In the real earth both density and wave speed tend to increase with depth. Furthermore, the depth of burial of a given device is dictated by containment requirements to be proportional to the cube-root of the expected yield. Thus, both (28) and (29) predict that the corner frequency will decrease less rapidly with yield than predicted by simple cube-root scaling.

B. Observations

1. Amplitude Scaling. Early experimental results seemed to support simple cube-root scaling. Gaskell [1956] performed several experiments in clay using small chemical explosives. The cavity size was found to be consistent with cube-root scaling, and the amplitudes of refracted waves were found to be proportional to the weight of the charge. O'Brien [1957, 1960] performed a regression analysis on three sets of data taken on small chemical explosions to determine the scaling exponent. The range of results was 0.88 to 1.12 with the mean value of 0.99±.18. Latter et al. [1959] found that at a Caltech seismic station located 180 km from NTS the recorded amplitudes were proportional to the first-power of yield.

Then the picture began to get clouded. O'Brien [1969] performed many experiments in sandstone and clay using chemical explosives with charge weights of 0.08 to 9.5 kg. Broadband measurements of radial stress were found to be dependent on yield to the 0.55 power in both materials, and a significant dependence on depth was also found. In clay the peak stress was found to decay as $h^{-0.38}$ and the half-period as $h^{-0.8}$. In sandstone, peak displacements were found to decay as $h^{-0.51}$ and half-periods as $h^{-0.61}$. Basham and Horner [1973] studying about 60 explosions, found Rayleigh waves to be proportional to the 1.2-power of yield from low yields to over 3 megatons. Springer and Hannon [1973] found the slope in the magnitude-yield relationship for body waves to be slightly greater than 0.6 at regional distances but to be almost 1.0 at teleseismic distances, while for Rayleigh-wave data they found the slope to be about 1.1. Murphy [1977] showed that the Mueller-Murphy model with its depth dependencies is consistent with: 1) the observed yield scaling exponents for large samples of NTS explosions below the water table using near-regional broadband spectra, 2) the broadband Rulison/Gasbuggy spectral ratio representative of explosions at very different scaled depths in hard-rock, 3) regional Pn amplitudes from NTS explosions and 4) both short-period and long-period teleseismic P wave spectra observed from a large sample of Pahute Mesa explosions covering the yield range from 155 to 1300 kt. Murphy also noted that the observed long-period surface wave data are inconsistent with the Mueller-Murphy model and suggested that there are factors contributing to the long-period, teleseismic surface waves which are not accounted for by the simple spherically symmetric source (or *isotropic*) models.

Marshall et al. [1979] studied a total of 46 explosions and found the slope for m_Q, a teleseismic body-wave magnitude, to be about 0.8 for US explosions below the water table in porous, saturated me-

dia and to be about 1.0 for US and USSR explosions in hard-rock. The slope for the surface-wave magnitude was found to be about 1.0. Larson [1982] found that the peak particle velocities measured in the laboratory from small chemical explosions in salt models could be cube-root scaled over 10 orders of magnitude of energy to those obtained from the SALMON experiment.

Lay et al. [1984] studied the Amchitka explosions, which were thought to have little tectonic release, so that long-period Rayleigh waves could be used without bias. They found that the Helmberger-Hadley [1981] source model is best fit if the long-period level of the explosion potential, ψ_∞, increases with yield, W, by $\psi_\infty \propto W^{0.90}$, or with yield and depth by $\psi_\infty \propto W/h^{1/3}$.

Nuttli [1986] found that the magnitude-yield relationship had a slope of about 0.7 for L_g waves. Patton [1988], applying Nuttli's method to a different data set, found that the slope was 0.95±0.03 for explosions in dry, porous material and 0.80±0.02 in saturated, porous material. Vergino [1989] found the slope to be 0.71 for 19 announced Soviet explosions. Vergino and Mensing [1990] found, after correcting for gas porosity, the slope in the magnitude-yield relationship to be 0.9 for a very large set of regional data for NTS explosions.

Finally, Patton (this volume) attempted to explain some of the differences in the scaling. He studied two classes of *non-isotropic* sources for NTS explosions: tectonic release and explosion-driven block motion. A non-isotropic source is one due to some non-spherically symmetric explosion-induced phenomenon. The main characteristic of tectonic release is that of strike-slip motions on faults at shot level or deeper while that of block-driven motion is mainly of vertical motion above the shot level, often in directions opposite to the naturally occurring faulting in the Basin and Range. In this analysis, he used fundamental and higher-mode surface-wave data recorded at regional distances and estimates of the spall source to invert the data into isotropic and non-isotropic components. From the estimates of the non-isotropic components, he tentatively concluded, pending further study, that there are two "fields" of explosions characterized by different non-isotropic mechanisms so that there is a reason for differences in scaling. For explosions above 300 kt, tectonic release with strike-slip faulting is a major contributor while for explosions below 300 kt block-driven faulting with reverse dip-slip motions is the major contributor. The result of the inversion process for the isotropic component gave reduced variance in the moment versus yield plots over those made without removing the spall contribution. In addition, the yield scaling exponent for explosions below the water table was reduced from about 1 to 0.84, i.e., closer to that expected from Mueller-Murphy model.

From the foregoing, there seems to be some reason to believe that the same scaling should apply to both long- and short-period data. There also seems to be a consensus building that simple cube-root scaling is not adequate in the real earth, though in the idealized world of laboratory models, it probably applies. Thus, some depth dependence such as in the Mueller-Murphy model is needed, but it is not clear whether some source material property or properties could be used to replace depth. And lastly, there seems to be a consensus that there is no curvature in the magnitude-yield relationship as predicted by Carpenter et al. and others. None of the investigations mentioned above found a need for anything but a straight line.

2. Corner frequency scaling. To aid in characterization of the source, Wyss et al. [1971] introduced the idea of *source dimension* (source radius) to explosions, $r_s = cv/f_c$ where c is a constant expected to be near unity and v is one of the elastic wave velocities. By introducing a constant of proportionality between the decay constant (ω_1 in (19)) and the boundary condition eigenfrequency, Mueller and Murphy [1971] obtained estimates of the elastic radius shown in Figure 4a. In the case of SALMON, the Mueller-Murphy estimate differs by about a factor of two from a recent estimate by a different procedure. The elastic radius estimated by Denny and Goodman [1990] is 460-520 m/kt$^{1/3}$ while the Mueller-Murphy value is about 270 m/kt$^{1/3}$. In contrast, the Denny-Goodman estimate of the source radius ($c = 1$ and $v = \alpha$) compares well with the Mueller-Murphy estimate as shown in Figure 4b. These results were obtained by removing the Mueller-Murphy constants of proportionality for tuff, rhyolite, shale and salt (1.5, 2.0, 2.4, and 4.5, respectively). The variance in the Mueller-Murphy scaled elastic radius plot is seen to be considerably greater than that in the scaled source radius plot. The scaled source radius plot also shows remarkable agreement between different materials. The significance of this may be that the mechanism that controls the generation of the corner frequency is nearly material-independent but that the one that controls the elastic radius is highly material-dependent. In either case, however, it is

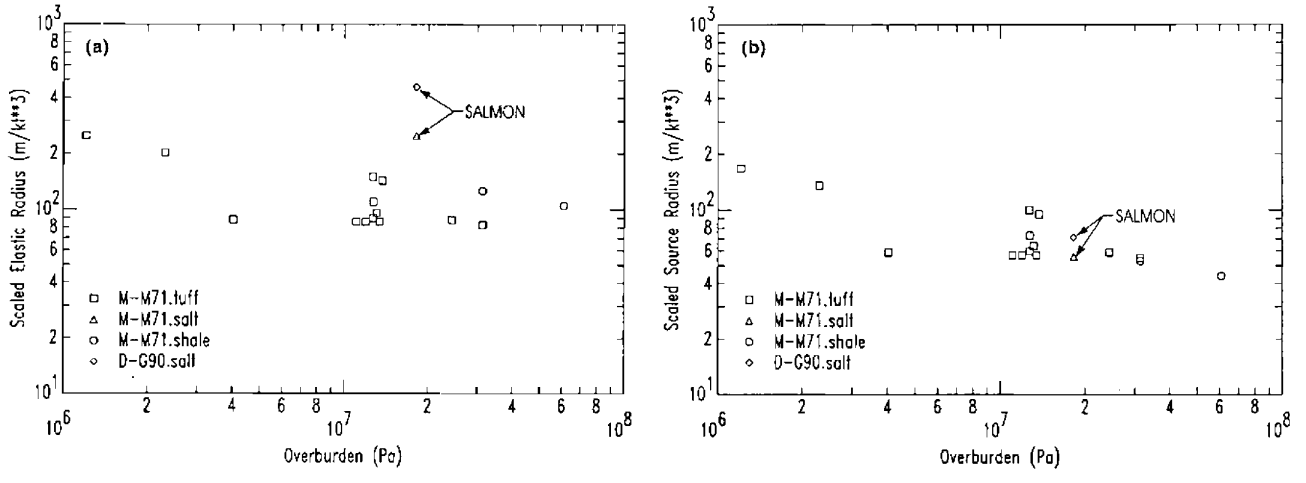

Fig. 4. Scaled radius vs overburden. (a) Elastic radius. (b) Source radius. (a) is Fig. 2 from Mueller and Murphy [1971] and shows that depth or depth-related changes in shot-point material properties are important. Mueller and Murphy presented their data as the elastic radius based on assumed constants of proportionality between the elastic radius and the corner frequency. Removing assumed constant from their data results in (b) a reduction in the variance; the two SALMON values are then nearly the same.

apparent that depth or some depth-related property plays a significant role.

As suggested above, the apparent depth dependence seen in Figure 4a and 4b may be due to some other parameter and depth is just a surrogate. Larson [1984] found in Nugget sandstone that the particle motion was always outward and did not return when the sample was unconfined but that it did return when confined. In other words, in the unconfined case the particle velocity was always positive and never negative as expected from (25). In salt, on the other hand, no difference was observed; the motion behaved basically as expected under both conditions. Clearly the corner frequency, one of the parameters which controls the response in (25), is dependent on the confining pressure for explosions in sandstone but not for salt. Figure 5a shows that the *shear strength* (i.e., half the difference in principal stresses) of salt is virtually independent of confining pressure while that of Nugget sandstone (Figure 5b) varies nearly linearly with confining pressure, suggesting that shear strength, not the confining pressure, is the real controlling parameter. One can, therefore, see that the corner frequency and the corresponding source radius could appear to be depth-dependent for some materials.

The source radius is also dependent on the wave-speed which, in general, increases with depth. Therefore, some of the trend, and perhaps some of the variance in Figure 4a and 4b, may be due to the wave speed. These observations are not to say that depth dependence is not important. In fact, Lay et al. [1984] found that the Helmberger and Hadley [1981] source model is best fit if the corner frequency parameter, K, scales as predicted by the Mueller-Murphy [1971] model. Clearly, the factors which control the corner frequency are not well understood and more work is needed.

C. Inferences from Dimensional Analysis and Other Considerations

As indicated above, the cavity volume should be an important scaling consideration. The same considerations that apply to cavity size should also apply to crater volume. Therefore, the dimensional analysis results of Chabai [1965] and others are worth reviewing. Chabai identified four different sets of scaling laws. If the gravitational field strength is not included in the dimensional analyses, then cube-root scaling is obtained when an explosion is characterized by either a mass dimension or by an energy dimension. If gravity is included in the dimensional analysis, then cube-root scaling is obtained for crater dimensions if the explosion is described by a mass dimension, but fourth-root scaling is obtained if the explosion is described by an energy dimension. Thus, in the last case, ground motion at low frequencies would be expected to be proportional to the three-fourths power of yield and at high frequencies would be proportional to the one-fourth power.

It was found experimentally that neither scaling law fit the crater data. Chabai did a regression analysis on chemical explosions ranging from 100 to 1,000,000 lb of TNT. He found that the data were fit best when scaled by 0.3 ± 0.02 power of energy. Baker et al. [1973; chapter 11] studied Chabai's data by combining the two basic dimensionless terms, $W^{1/3}/\sigma^{1/3}d$ and $W^{1/4}/K^{1/4}d$ where W is an energy dimension, d is the depth, K represents the dead weight of the material, best measured by ρg, and σ represents the material strength. They found that the crater-radius, R_c, data were fit very well by

$$\frac{R_c}{d} \propto \left(\frac{W^{1/3}}{\sigma^{1/3}d} \times \frac{W^{1/4}}{K^{1/4}d}\right)^{1/2}. \tag{30}$$

They suggest that the material strength is best measured by ρc^2, an easily determined quantity, but it could just as well be some other measure. From this analysis, the authors concluded that neither the gravitational effects nor the constitutive effects can be ignored. For the seismic source function, this is an interesting result. It can be seen from (30) that depth cancels out and that the volume scales as yield to the 7/8 power. Thus, the volume has no explicit depth dependence and the yield scaling is remarkably close to that commonly observed for seismic amplitudes!

Working with small models in the laboratory, Larson [1984] found that cavity volumes produced by explosions vary inversely with shear strength and are dependent on confining pressure only to the extent that the shear strength depends on confining pressure. In salt, for example, the shear strength is independent of confining pressure, but in Nugget sandstone it is nearly linearly dependent on it as shown previously in Figure 5. Thus, instead of ρc^2 for σ in (27), Larson's work would suggest that shear strength be used. Larson further concluded that relationships such as that of Orphal [1970] which are explicitly dependent upon depth of burial may work well in certain media (e.g., very weak fluidlike media or in media where shear strength increases proportional to depth); but extrapolation of such a relation to other materials, and in particular to salt, would be extremely dangerous.

It is also worth noting that according to Crowley [1970] cube-root scaling only applies if, in addition to gravity, radiation effects are not an important consideration. If either is a significant consideration, then according to Crowley scaling is no longer possible. In addition, Glenn [1990] shows that cube-root scaling is strictly valid only if a point source explosion is considered. For a finite source, two addi-

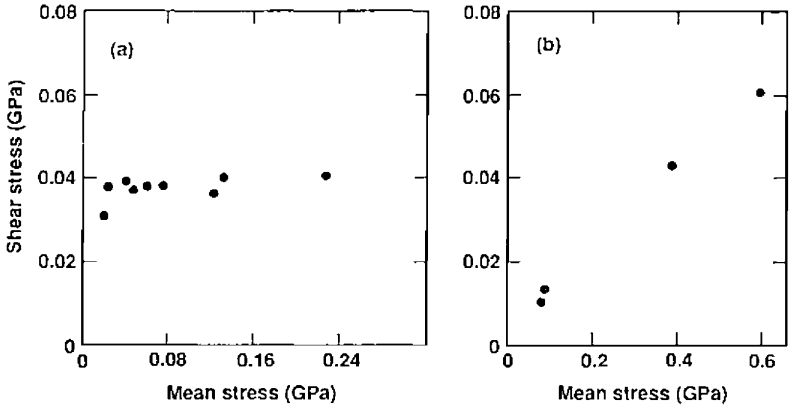

Fig. 5. Shear strength versus confining pressure [Larson, 1984]: (a) salt and (b) Nugget sandstone. In salt the shear strength is independent of confining pressure while in Nugget sandstone shear strength is nearly linearly dependent on it.

tional parameters, the mass and energy per unit volume, enter the problem via the initial conditions. Glenn then points out that with nuclear explosives, the experimental emplacement cannister generally bears little relation to the yield and shows how this manifests itself in the amount of internal energy deposited in a material. Holding the source volume fixed, while varying the yield, Glenn's calculations showed that cube-root scaling is only a crude approximation. Thus, there are reasons why cube-root scaling may not be appropriate to the seismic source function.

V. New Directions: Chemical/Nuclear Equivalence

There has long been a concern that chemical and nuclear explosions can not be scaled to each other and that free-field measurements are also somehow different from measurements made at greater distances. These concerns are addressed in this section. New regression analysis results are reported for cavity size, seismic moment, and corner frequency. The compilation of data include previously published and unpublished data from both nuclear and chemical explosions and from all measurement regimes. The data, whether measured in the free-field or at teleseismic distances, did not reveal any differences between chemical and nuclear explosives for the basic source function parameters.

A. New Regression Results

As described above, Mueller and Murphy [1971] and Murphy [1974 and this volume] have presented a theoretical relationship of seismic moment to cavity size and have demonstrated some experimental evidence in support of it. They have also shown that the scaled corner frequency is depth-dependent. In the following, the relationship of cavity size to seismic moment is expanded to include corner frequency. The analysis consists of two phases. Initially, an empirical model is fit to the data (cavity radius, seismic moment, and source radius) to determine if the data are consistent with the theoretical yield scaling. Since the data do not contradict the theoretical scaling, the yield exponent (coefficient in log space) is fixed at the theoretical value. Had the empirical coefficient been significantly different from the theoretical value, the empirical value would have been adopted.

The second phase of the analysis is to select the most parsimonious model which includes the effects of parameters, other than yield, which explain the variation in the observed data. Coefficients for the parameters included in the model are estimated using the standard regression technique of minimizing the sum of squared differences between the observed data and the model. In addition to estimating the coefficients, two other outputs of the regression analyses were used to compare alternate models. One, the estimated standard deviation, σ, of the measured variables was used to compare two models with the same number of parameters. The model with the lowest value of σ is preferred. The second output, the significance level, p, associated with each parameter, was used to test the importance of each parameter. If the significance level is low, e.g., $p \leq 0.05$, the parameter was considered to explain a significant amount of the observed variation in the measured variable and is retained in the model. On the other hand, if the significance level is large, e.g., $p \geq 0.05$, the parameter is not considered to explain a significant amount of variation above that explained by the other parameters in the model and is dropped from the model. The final model consists only of statistically significant parameters.

All of the models considered below consist of products of parameters raised to some power. When written in logarithmic form, all but one of these models become linear with the original exponents as coefficients. The random variation associated with the measured variables, after fitting the model in log space, is expressed, in its original units, in terms of an *F-value* corresponding the 2σ level of variation in log space, i.e.,

$$F_{2\sigma} = 10^{1.96\sigma}, \tag{31}$$

where σ is the standard deviation derived from the regression analysis. The F-value could just as well be defined at the 1σ level by omitting the 1.96 factor in (31). The F-value is frequently used to construct confidence interval estimates of the 'true' value of the response (e.g., cavity radius, seismic moment, or source radius) given a fixed yield and fixed values of the other parameters in the model. For example, if $F_{2\sigma} = 1.3$ and x is the predicted value of the cavity radius, then the true cavity radius can be expected with 95% confidence to be between $1.3x$ and $x/1.3$.

1a. Cavity Size—Theory. Under the assumption that the material's shear strength is negligible, Nuckolls [1959] derived a solution for the cavity radius

$$R_c = CW^{1/3}/P_0^{1/3\gamma}, \tag{32}$$

where γ is the adiabatic expansion coefficient of the cavity gas, P_0 is the overburden pressure ($P_0 = \rho gh$), and C is a function of γ, the vaporization pressure, and of a proportionality constant relating energy to the product of cavity gas pressure and volume ($PV \sim E$). Each of these parameters is material-dependent. Haskell [1961] found an implicit, quasi-static solution to the cavity problem for an elastic, plastic material which behaves according to the Coulomb-Mohr criterion, i.e., the shear strength is a linear function of the confining pressure plus a constant. The parameters in this solution are initial cavity radius, elastic radius, Lamé constants, overburden, γ, yield, and shear strength quantities. In both cases, depth enters the problem by way of the overburden pressure.

Boardman et al. [1964] and Higgins and Butkovich [1967] estimated the material dependent constant, C, in (32) for several materials. Boardman et al. assumed that $\gamma = 4/3$ and had data from 35 explosions available while Higgins and Butkovich evaluated γ as well as C for several materials using 46 explosions. Both groups reported excellent results for these small data sets; Boardman et al. had a 2σ F-value of about 1.15 to 1.47 depending on material while Higgins and Butkovich had less than 1.22, with γ ranging from 1.013 to 1.142 depending on source material. Higgins and Butkovich concluded that cavity size is independent of the material's shear strength.

Closmann [1969] performed a regression analysis on the same 46 nuclear explosions and estimated the coefficients in the empirical cavity radius, yield, and material properties relationship,

$$\log(\hat{R}_c/h) = x_0 + x_1 \log(W^{1/3}/h\kappa^{1/3}) + x_2 \log(\mu/\kappa) + x_3 \log(\mu/P_0), \tag{33}$$

to be 0.131, 0.918±0.037, -0.820±0.674, and 0.244±0.037 for x_0 through x_3, respectively, where κ is Young's modulus. After collecting terms (33) becomes $R_c \propto W^{0.306}/h^{0.161}$. He did not report on the statistical significance of these coefficients but did recognize that the large standard deviation on x_2 did indicate a large uncertainty in its use. Had he dropped this pair of terms and recalculated the remaining coefficients, he may have found somewhat different yield and depth exponents. He neither did this nor did he offer any justification for retaining this term.

Other investigators [Michaud, 1968, Orphal, 1970, Terhune and Glenn, 1977 and Glenn, 1991] have attempted to include the material's shear strength. Michaud simply modified (32),

$$R_c = \frac{52C}{(P_0 + C_s)^{1/3\gamma}} W^{1/3}, \tag{34}$$

where C refers to the emplacement geometry ($C = 1$ for a tamped explosion) and C_S is a strength term. Orphal derived the cavity size for an elastic, plastic material using the Coulomb-Mohr yield criterion and a simplified cavity pressure assumption to obtain an explicit solution for the cavity radius,

$$R_c = \frac{C_1}{((C_2 + P_0)^n - C_2)^{1/3\gamma}} W^{1/3}, \quad (35)$$

where C_1 is a function of vaporization radius and pressure, while C_2 and n are different functions of the shear strength parameters and Young's modulus.

Terhune and Glenn [1977] performed a parameter study using 1- and 2-dimensional finite differences codes to determine a functional relationship of cavity size to overburden, shear strength, and yield. They assumed that the material's shear strength can be modelled by a combination of the Coulomb-Mohr and the von Mise's yield criteria, i.e., the shear strength is linearly proportional to confining pressure (Coulomb-Mohr) up to some point but beyond that it is constant (von Mise's). The results indicated that cavity radius is determined by

$$R_c = \frac{63\ W^{7/24}}{P_0^{1/12}\ Y^{1/4}}, \quad (36)$$

where Y is the shear strength. The yield exponent of 7/24 was determined by plotting the difference between the final and initial cavity sizes versus yield. From this, they concluded that the yield scaling (7/24) of Baker et al. [1973] applies.

Following Haskell [1961], Glenn [1991] found a quasi-static solution using von Mise's yield criterion. This solution is also an implicit one. However, an explicit solution is possible in the case where the cavity's final size is much larger than its initial size, as in a nuclear explosion. The cavity radius is then

$$R_c = C\left[\frac{3(\gamma - 1)}{4\pi(P_0 + \frac{2}{3}YF)}\right]^{1/3\gamma} W^{1/3}, \quad (37a)$$

where

$$F = 1 + ln\left[\frac{2\mu}{3Y}\left(\frac{1+\nu}{1-\nu}\right)\right], \quad (37b)$$

and C depends on the initial cavity size.

Using (35), Orphal [1970] analyzed 172 explosions but he had estimates of the required material properties, including γ, only for broad categories of materials. He found that cube-root scaling was not significantly different from the 0.29 obtained by Heard [reported and used by Mueller and Murphy, 1971] and that the depth exponent ranged from 0.08 to 0.14 depending on media.

Yield and depth exponents are important quantities in the seismic moment versus yield (or cavity size) relationship and the difference between 0.29 or 0.306 and 1/3 can be important. For example, the use of Heard's cavity radius yield exponent by Mueller and Murphy [1971] results in an amplitude, yield scaling exponent of 0.87, considerably less than the theoretical value of 1. Therefore, these exponents should be as well determined as possible. Since Orphal's work was published, cavity data and some corresponding material properties data (but unfortunately not shear strength) have become available on nearly twice as many explosions, therefore, the empirical cavity size versus yield relationship was re-evaluated, incorporating available material properties.

1b. Cavity Size—Regression Analysis. The theoretical relationships (32), (34), (35), and (37a) all predict a cube-root yield dependency. Only the finite difference parameter study of Terhune and Glenn [1977] predicts a different yield dependency. Of those that incorporate shear strength, only (36) has it as a stand-alone term; the others all have it combined with overburden. If γ is significantly different for each material then (32), (34), and (35) predict different depth dependencies. Therefore, one issue to be addressed, in addition to whether the data support cube-root scaling, is the correct functional form to include shear strength. Another is whether the data support different depth dependencies for each material. To address these issues, the US cavity data and geophysical parameters in the LLNL Nuclear Test database [Howard, 1983] were used, supplemented with data from 4 French tests in granite and 1 USSR test in salt [Lin, 1978] and with data from laboratory experiments in salt and sandstone [Larson, 1984].

As shear strength is not one of the parameters in the database, the second of the above questions cannot be fully addressed. However, relationships of the quasi-static form (34, 35, and 37a) can probably be ruled out. The parameters γ and Y of (37a) were found by non-linear regression analysis. While the value found for Y (10 MPa) was reasonable, the one for γ (0.2) was not. This should not be too surprising since Glenn [1991] also found that the quasi-

TABLE 2. Cavity Radius

2.1 $\sigma = 0.0734$
N = 358
$F_{2\sigma} = 1.393$

Parameter	Coeff.	Std. error	p
Intercept	3.9906	0.3819	0.0000
W	0.3397	0.0021	0.0000
ρ	0.2433	0.1395	0.0820
μ	-0.1807	0.0273	0.0000
P_0	-0.2787	0.0295	0.0000
GP	-0.0020	0.0008	0.0188

2.2 $\sigma = 0.0742$
N = 358
$F_{2\sigma} = 1.393$

Parameter	Coeff.	Std. error	p
Intercept	4.1028	0.3843	0.0000
ρ	0.2185	0.1408	0.1216
μ	-0.1950	0.0272	0.0000
P_0	-0.2621	0.0293	0.0000
GP	-0.0024	0.0008	0.0041

2.3 $\sigma = 0.1151$
N = 358
$F_{2\sigma} = 1.679$

Parameter	Coeff.	Std. error	p
Intercept	4.8407	0.5959	0.0000
ρ	0.0554	0.2183	0.7998
μ	-0.2890	0.0422	0.0000
P_0	-0.1527	0.0455	0.0009
GP	-0.0053	0.0013	0.0001

2.4 $\sigma = 0.0741$
N = 358
$F_{2\sigma} = 1.397$

Parameter	Coeff.	Std. error	p
Intercept	4.1667	0.1793	0.0000
β	-0.3848	0.0467	0.0000
P_0	-0.2625	0.0292	0.0009
GP	-0.0025	0.0008	0.0016

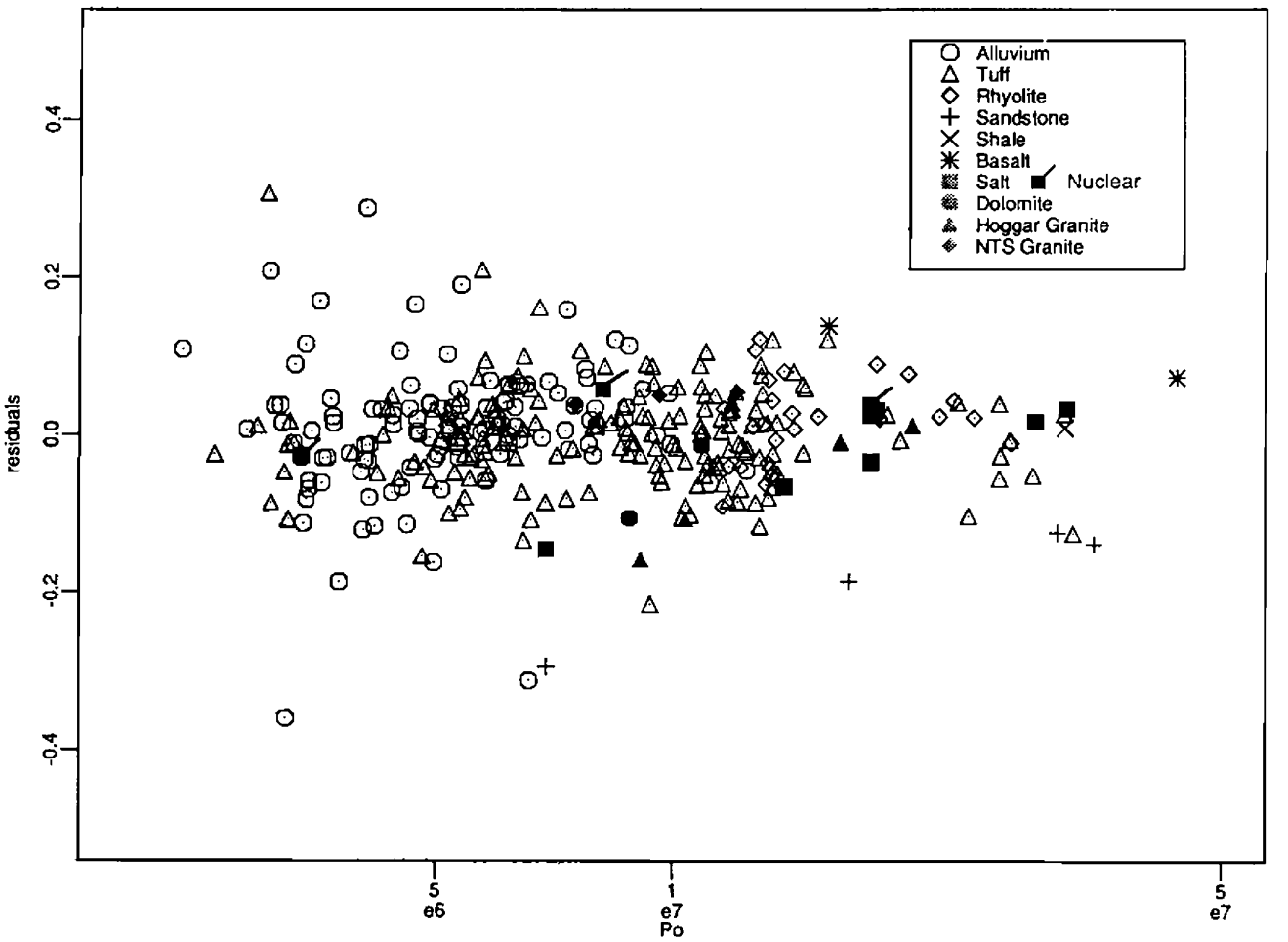

Fig. 6. Cavity radius residuals versus overburden. The sandstone and the unflagged salt data are from very small laboratory chemical explosions [Larson, 1984]. No clear evidence is seen to support a different depth dependence for each material and no clear evidence is seen that chemical explosions are different than nuclear ones. A shear strength and a tamping factor are probably required to explain the remaining variance.

static solution approximated the dynamic one only when the cavity's final radius was not much larger than its initial radius. This is clearly not the case for a fully tamped nuclear explosion and, therefore, (37a) does not apply. A relationship incorporating shear strength as in (36) is more likely to be appropriate.

To address the yield scaling issue, a log-linear model similar to (30) and (33) was used:

$$\log \hat{R}_c = x_0 + x_1 \log W + x_2 \log \rho + x_3 \log \mu + x_4 \log P_0 + x_5 GP, \quad (38)$$

where GP is the gas-filled porosity, i.e., that portion, given in percent, of the total volume filled with gas. The gas porosity was included because Butkovich [1976] found, when investigating the disposition of the former cavity material, that even 1% gas porosity can account for the total cavity volume in just a few cavity radii if the pores are completely crushed. The density and shear modulus were included because a preliminary investigation of cube-root scaled cavity radii showed that both it and gas porosity could explain much of the variance.

The intercept, x_0, and coefficients, x_i, of (38) were found and are given in Table 2 as model 2.1. Based on the criteria given in the introduction to this section, the significance levels indicate that all the variables except density make a significant contribution. The estimated yield coefficient clearly suggests cube-root as opposed to 7/24 scaling of Baker et al. Nevertheless both scaling laws were tested by running two additional models. The yield coefficient was set to 1/3 and 7/24 in model 2.2 and 2.3, respectively, and the other coefficients were re-evaluated. The results are shown in Table 2. Of the two models. 2.2 has a much smaller standard deviation and corresponding F-value. Therefore, the data do support cube-root rather than Baker et al. scaling.

While the significance level in model 2.2 suggests that the density does not make as significant contribution to the reduction of the variance over that of the other variables, its coefficient and that of the shear modulus are nearly the same value but of opposite sign, suggesting that both of them could be replaced with shear wave velocity. This possibility was tested in model 2.4 and was found to fit the data equally well. Since 2.4 is a smaller model, it is preferred over 2.2.

The residuals of model 2.4, shown in Figure 6 versus overburden, address the depth dependence and chemical versus nuclear questions. If the various materials have different depth dependencies it is not

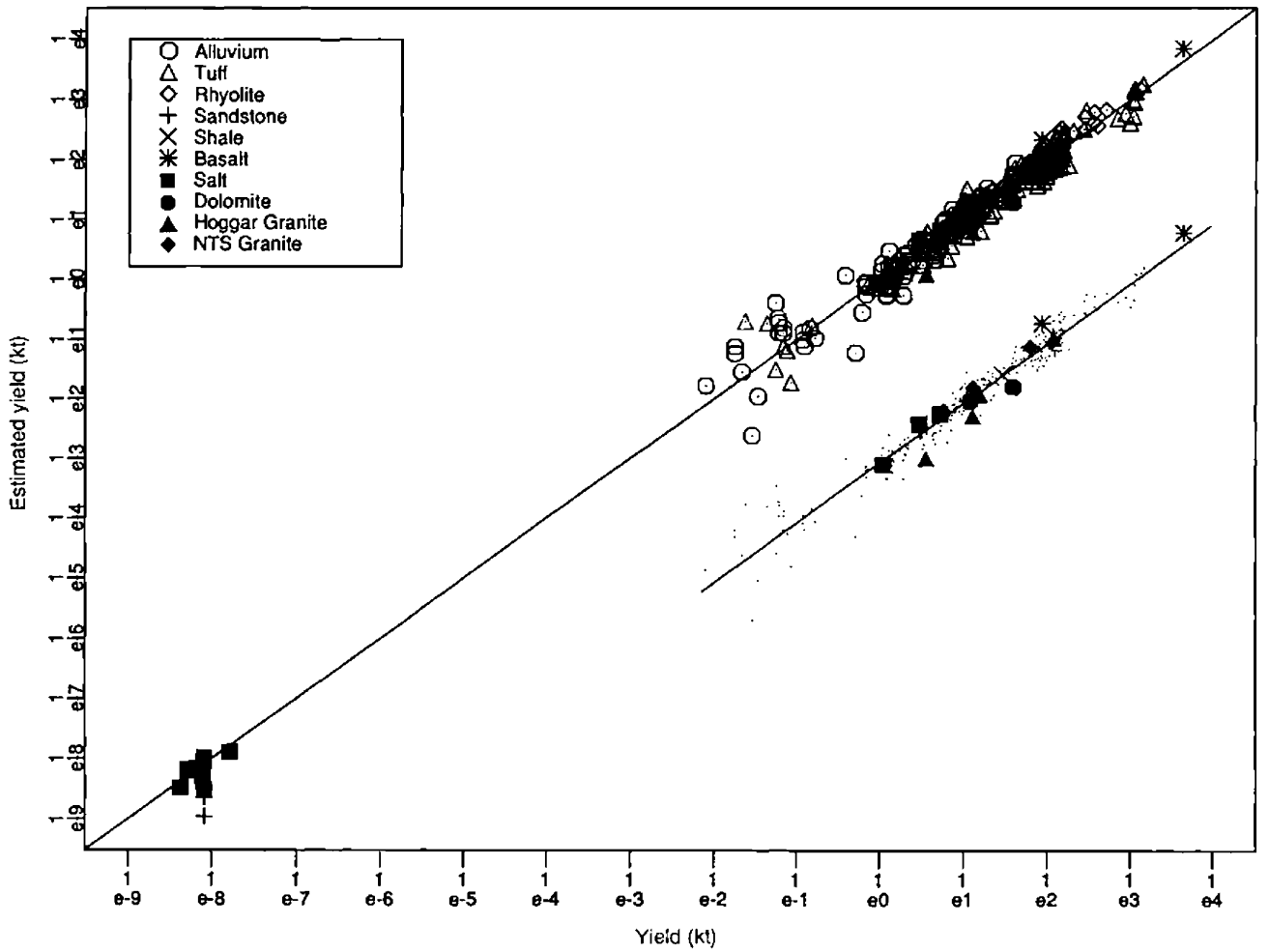

Fig. 7. Estimated yield from (39) vs actual yield. The very small chemical explosions ($W < 1\times10^{-7}$ kt) are as well estimated as the nuclear ones. The reduction in the variance due to (39) is large at nuclear yields greater than about 1 kt but not at lower ones. This is probably due to measurement error. The hard-rock explosions randomly overlay the ones in porous rock as seen in the offset where the highly porous rocks are not differentiated.

clearly evident. The hard-rock materials exhibit as much variance as the porous ones. Nor is it clear that chemical explosions are different from nuclear ones since the chemical explosions in salt appear to merge with the nuclear ones at high overburden (taken to be the same as confining pressure in this figure). Apparently to explain the remaining variance in Figure 6, shear strength, and possibly initial cavity size, must be taken into account. As Glenn [1990] points out, the emplacement cannister size bears little relation to yield. Therefore, a tamping factor as well as a shear strength term may be required in (38). If such information could be made available, (38) should be appropriately modified and re-evaluated.

Given model 2.4, the cavity radius, yield relation is

$$\hat{R}_c = \frac{1.47\times10^4\ W^{1/3}}{\beta^{0.3848}\ P_0^{0.2625}\ 10^{0.0025GP}}. \qquad (39)$$

Several interesting results of (39) can be seen in Figure 7. The yields of the laboratory chemical explosions are as well estimated as those of the nuclear ones. Also seen is that the variance about (39) is largest for the low nuclear explosions. This may be due to the measurement error, estimated to be about 1.5 meters (N. R. Burkhard, LLNL, per. comm.). The most significant aspect of Figure 7, however, is that the hard-rock explosions randomly overlay the porous ones.

2. Seismic Moments. In Figure 8 seismic moments are plotted against yield. The measurements were made in all distance regimes, for both types of explosions, and in many different types of materials. No distinction is made between the different types of data and it is not clear that they are consistent with each other or with yield scaling to the first power. To unify the data, the ratio of the measured moment to the theoretical moment was modelled with

$$\log(\hat{M}_0/M_t) = x_0 + x_1 \log W + x_2 \log\mu + x_3 \log P_0 + x_4 GP, \qquad (40)$$

where $M_t = \frac{4}{3}\pi\rho\alpha^2\hat{R}_c^3$. The coefficients in (40) were evaluated with and without the data of Aki et al. This was done because of the concerns stated above that the free-field moments may have been estimated from data taken in the non-linear region and that the other moments may include effects due to non-isotropic mechanisms, e.g., tectonic release or driven block motions. Using the same procedure outlined above, virtually identical results were found for the two cases. The shear modulus was not found to contribute to the reduction in variance while overburden and gas porosity were. It

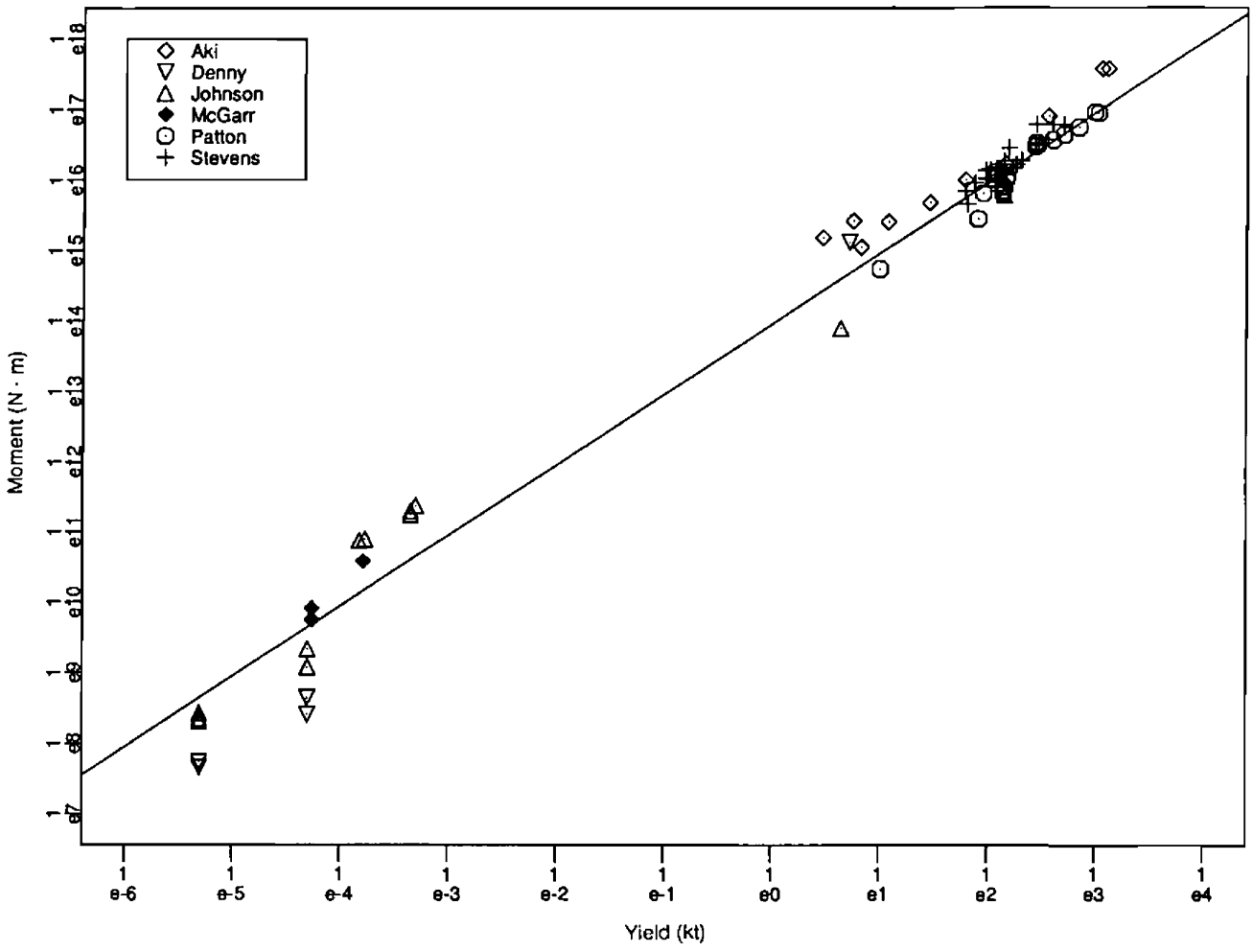

Fig. 8. Moment vs yield. The small explosions ($W < 0.001$ kt) are chemical and the others are nuclear. The data of Aki et al. [1974] and Patton (this volume) were previously described. The data of Johnson are from moment tensor inversions of surface data taken close-in on (1) the small chemical explosions at NTS [Johnson and McEvilly, 1990], (2) chemical explosions fired by the USGS in a limestone quarry [McEvilly and Johnson, 1989], and (3) two nuclear explosions at NTS [Johnson, 1988]. McGarr and Bicknell [1990] took their data both in the free-field and close-in on the surface from chemical explosions in two South African gold mines. The data of Denny [1990] include SALMON and free-field measurements of chemical explosions at NTS (unpublished). The data of Stevens [1986] are from measurements of teleseismic surface waves.

was also found that no additional yield term is required. The yield dependency contained in M_t, first power from (39), is sufficient. The model obtained for the seismic moment is

$$\dot{M}_0 = \frac{1}{311} M_t P_0^{0.3490} 10^{-0.0269GP} \tag{41}$$

The reduction in variance due to (41) over a simple moment, yield relationship can be seen by comparing Figure 9 with Figure 8. This comparison shows a very large reduction, especially at the very low yields where the range in gas porosity is the greatest. A large reduction is also seen in Aki's data set. Figure 9 demonstrates that there is probably no need to treat the different kinds of materials separately, as the hard-rock explosions overlay the porous ones.

That the different types of data, i.e., chemical, nuclear, free-field, close-in, regional, and teleseismic, appear to be consistent can be seen in Figures 9 and 10. If there were an important difference between the different types, it is not evident in these figures. In Figure 9, the chemical explosions are as evenly distributed about the simple moment, yield regression line as the nuclear ones, and in Figure 10 the measurement regimes, likewise, seem to be compatible with each other.

It is important to bear in mind that, although the total number of measurements is 86, the data set is not large considering its diversity. It is well known that statistical results on small data sets can be misleading and the F-value, in this case, is not small. Therefore, these results should not be taken as an unequivocal demonstration of the compatibility of the different data types. More data may change the picture. Nevertheless, there is no indication of a difference between the various types of data. Efforts should be made to enlarge the data set and, especially, to fill in the huge gap near 1 kt.

3. Corner Frequency/Source Radius. The data used in the corner frequency analysis are shown in Figure 11, where instead of corner

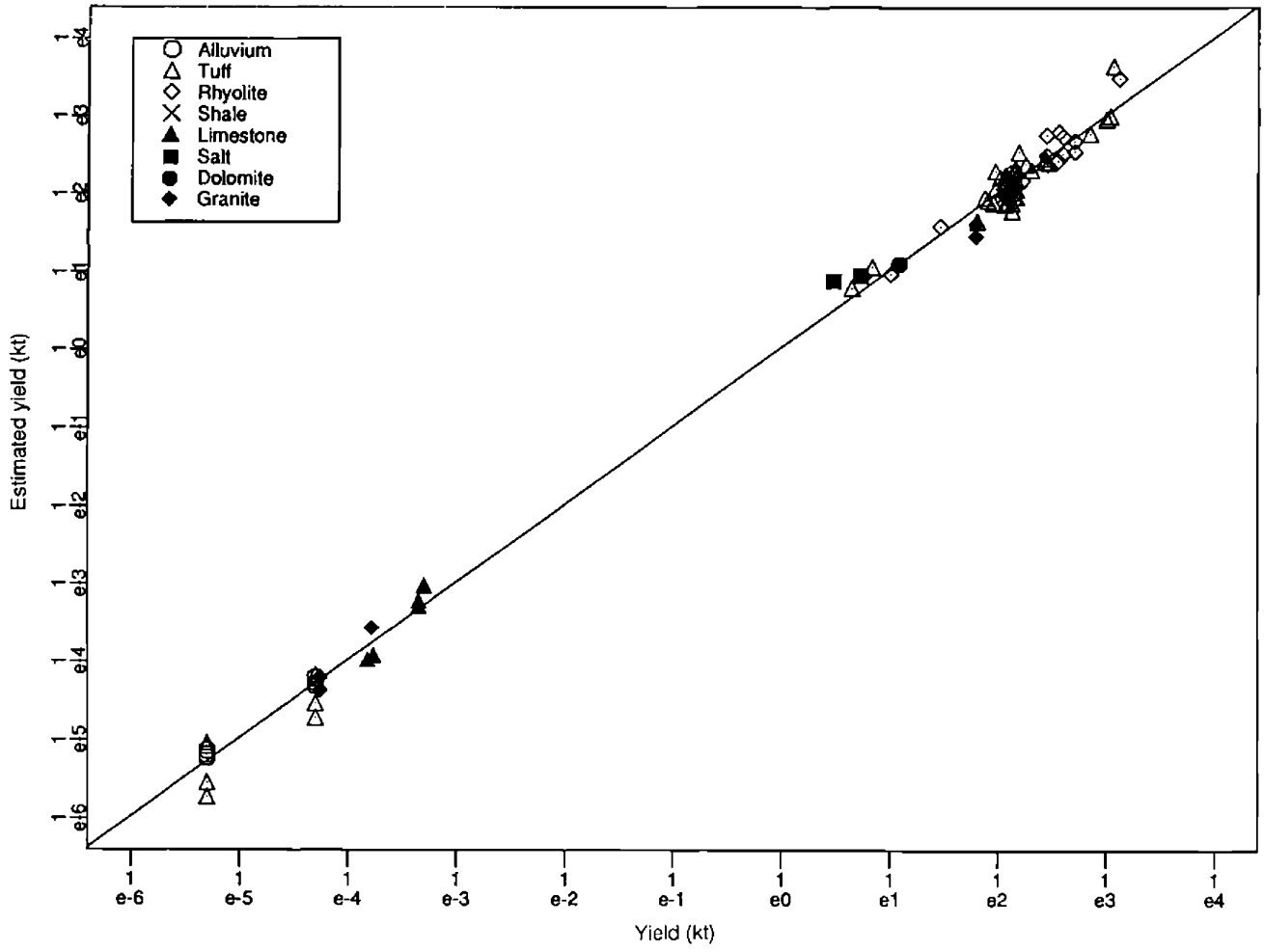

Fig. 9. Yield estimated from (41) versus actual yield by material. As with the cavity radius results, the hard-rock moments randomly overlay those for porous rocks. Also the chemical explosions are seen to be consistent with the nuclear ones. The reduction of variance due to (41) over a simple moment, yield relationship can be seen by comparing this figure with Fig. 8. The 95% confidence level F-value is 6.34 for Fig. 8 while in this figure it is 2.34.

frequency, source radius, $R_s = \beta/\pi f_c$, has been plotted. This figure shows that the different types of data appear to be consistent with each other and with cube-root scaling. This would not be the case if attenuation had an important effect on the data. To confirm cube-root scaling, the ratio of the measured source radius to the cavity radius was modelled with

$$\log(\hat{R}_s/\hat{R}_c) = x_0 + x_1 \log W + x_2 \log \rho + x_3 \mu + x_4 \log P_0 + x_5 GP \quad (42)$$

where R_c is given by (39). No additional yield term was found to be required. The yield dependency contained in R_c, cube-root, is sufficient. Both the shear modulus and the overburden were found to make significant contributions to (42) but density and gas porosity were not. The model for source radius is

$$\hat{R}_s = \frac{1}{9443} \hat{R}_c \mu^{0.7245} P_0^{-0.2897}. \quad (43)$$

The reduction in variance due to (43) over a simple source radius, yield relationship can be seen by comparing Figure 12 with Figure 11. This comparison shows that (43) reduces the variance considerably but not as dramatically as in the moment case. As with the moment data, the few hard-rock (Figure 12) explosions randomly overlay the porous ones with the exception of the one in salt (SALMON). Also, as with the moment data the different data types (Figure 13) appear to be consistent. Finally, there has been concern that corner frequency estimates from data taken outside of the free-field are contaminated by spall [Vergino et al., 1988]. While this phenomenon undoubtedly occurs, it does not appear to be a serious problem, given the variance in the data.

This data set is half again larger than the seismic moment set and, therefore, it may provide somewhat greater confidence that no significant differences between the various types of data exist. However, efforts should still be made to enlarge the data set and to fill in the huge gap near 1 kt.

B. Conclusions

Of the source model parameters, the seismic moment and the corner frequency are better known than the roll-off or the overshoot.

The empirical cavity radius formula, (39), found in this study is significantly different from that used in the Mueller-Murphy source model and leads to different yield scaling. The source function's mo-

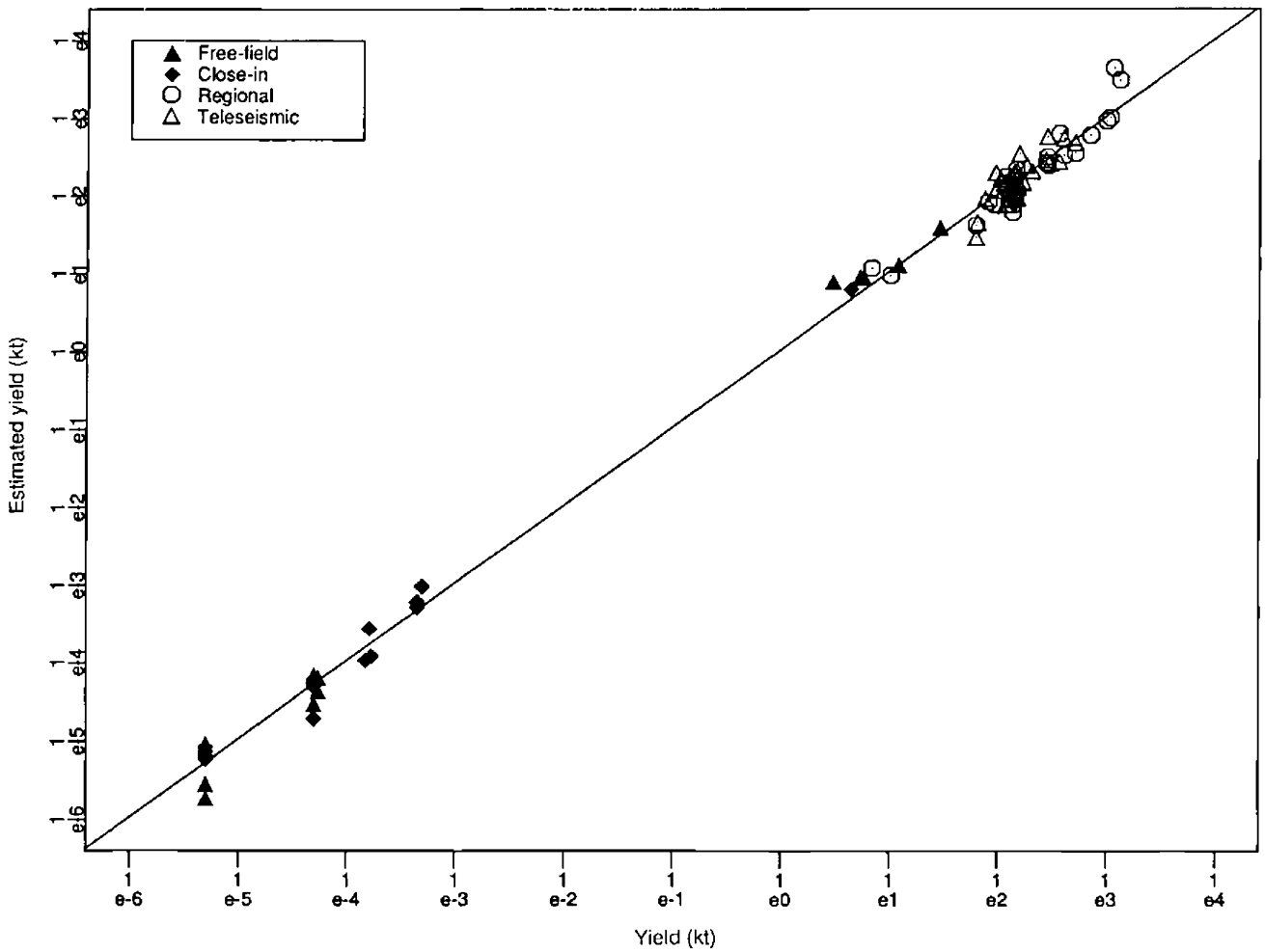

Fig. 10. Yield estimated from (41) versus actual yield by measurement regime. The various regimes are indistinguishable as they are randomly interspersed.

ment and corner frequency are both dependent on the cavity radius, but in different ways, and are consistent with cube-root scaling when the material properties are taken into account. All three of these source properties are seen from (39), (41) and (43) to be dependent on depth of burial. Unfortunately the question of whether depth is a surrogate for shear strength, as suggested by Larson's [1984] work, could not be addressed as shear strength data is not available on a case by case basis. However, Schock [1981] has presented data that show a rough correlation between yield strength and shear wave speed, suggesting that perhaps shear wave speed is a surrogate and depth is not.

No evidence was found in this study to suggest that chemical and nuclear explosions are significantly different. In fact, the data support the conclusion of Killian et al. [1987] who found from a comprehensive finite difference study of nuclear and chemical explosions in a variety of geologic materials that no differences between the two sources exists beyond a range equal to twice the original size of the chemical explosive.

C. Implications

Assuming that (39), (41), and (43) are a perfect representation of reality, then some interesting consequences can be derived. If the material properties are independent of depth and the containment rule requires that depth be proportional to the cube-root of the yield, then cavity radius, moment, and corner frequency would scale as $W^{0.246}$, $W^{0.849}$, and $W^{-0.148}$, respectively. A more realistic picture for NTS can be formed by calculating the source function properties for all the explosions having the required material properties. The results of this sampling of NTS suggest that, given only the yield, cavity radius can be estimated to within a factor of 1.6 with 95% confidence. Similarly, seismic moment, corner frequency, and energy can be estimated within a factor of 4.9, 1.7, and 6.4, respectively. To obtain a smaller F-value, the material properties must be tightly controlled.

The results of the above calculation are shown for seismic moment and corner frequency in Figures 14 and 15, respectively. The slope is seen to change significantly with increasing yield in both figures. This is due to the material property changes with depth (yield). Given this large variance and character of the moment plot, it is not difficult to see how repeated random samplings of these results for a small number of explosions could produce greatly different slopes. The many different observations, documented above, are then not surprising.

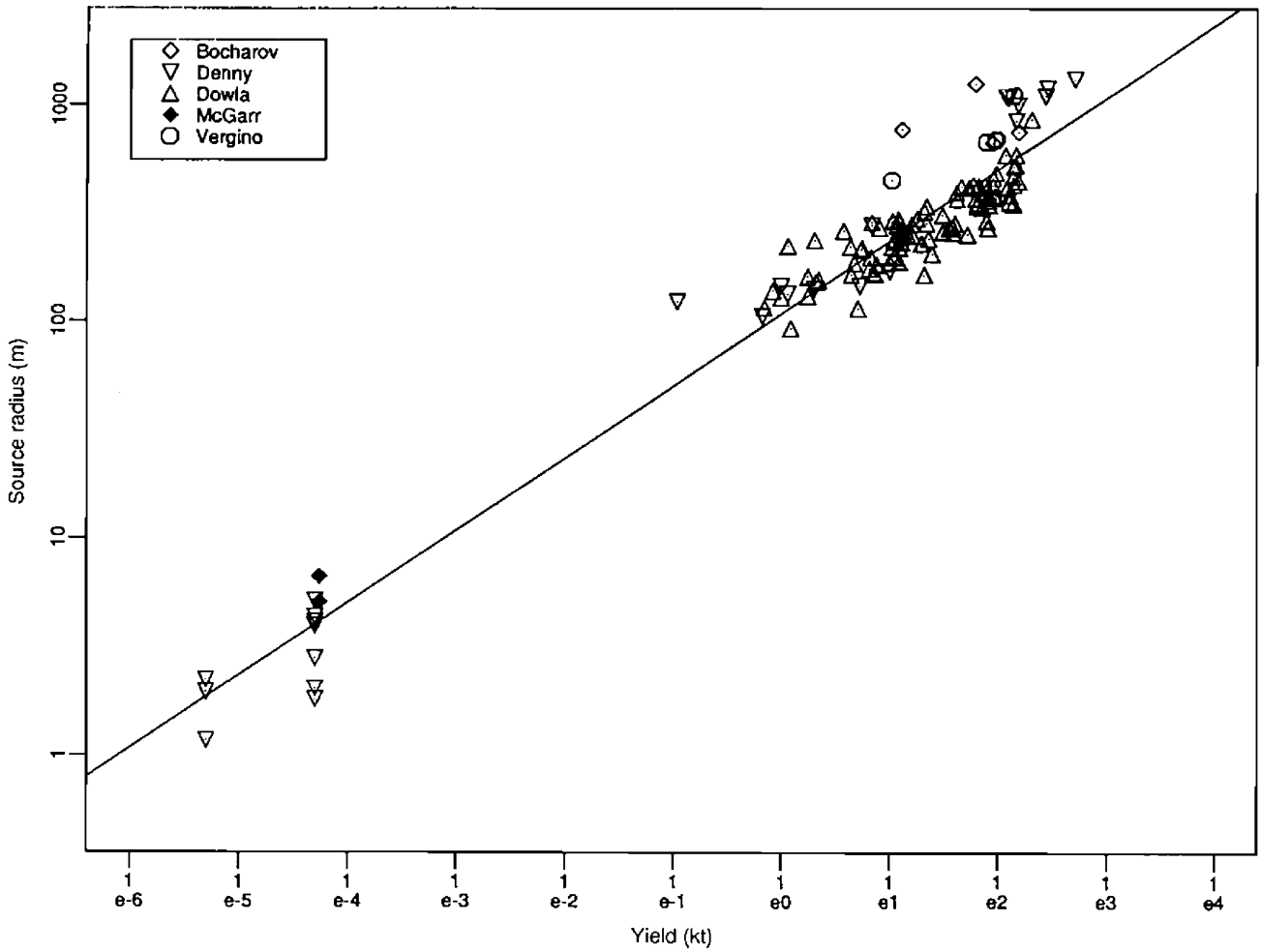

Fig. 11. Source radius versus yield. The small explosions are chemical ones while the remainder are from nuclear explosions. The data of Bocharov et al. [1989] are from a single broadband, teleseismic station and were estimated from the peak of the particle velocity spectra. The data of Denny are from (1) free-field and close-in measurements of chemical explosions at NTS (unpublished) and (2) from peaks of station averaged particle velocity spectra of regional measurements (unpublished). The data of Dowla (per. comm.) are from regional measurements made by fitting the P_g displacement spectra with a second order model. McGarr and Bicknell [1990] estimated the corner frequencies from the particle velocity spectra from free-field and close-in surface measurements described above. Their surface datum was omitted because it apparently suffered a great deal of attenuation traveling upward in the crust. The data of Vergino et al. [1988] were from regional measurements reduced by the transfer function technique, e.g. see Denny and Goodman [1990].

VI. Summary and Recommendations

The vibrating sphere problem provides a good starting point for building a model for the seismic source function of underground explosions. However, little is known about the basic properties of the radial stress and elastic radius. Instead, the parameters of moment, corner frequency, overshoot, and roll-off are estimated to describe the source function. A source radius term can be defined from the corner frequency but it has no known relationship to the elastic radius except that, in a fully tamped explosion, it is greater than the elastic radius, while in a fully decoupled explosion, it is equal to the elastic radius.

An interesting, worthwhile exercise would be to derive the equivalent radial stress for those few explosions where free-field radial particle velocity measurements were made at several ranges. For those explosions whose data are only in the non-linear zone, the results would obviously be fictitious but their progressive change in shape with range may be enlightening.

In this study it was found that the seismic moment and the corner frequency are better known than the other source properties, though not so well known that additional data would not increase confidence in the empirical formulas. On the contrary, additional data should

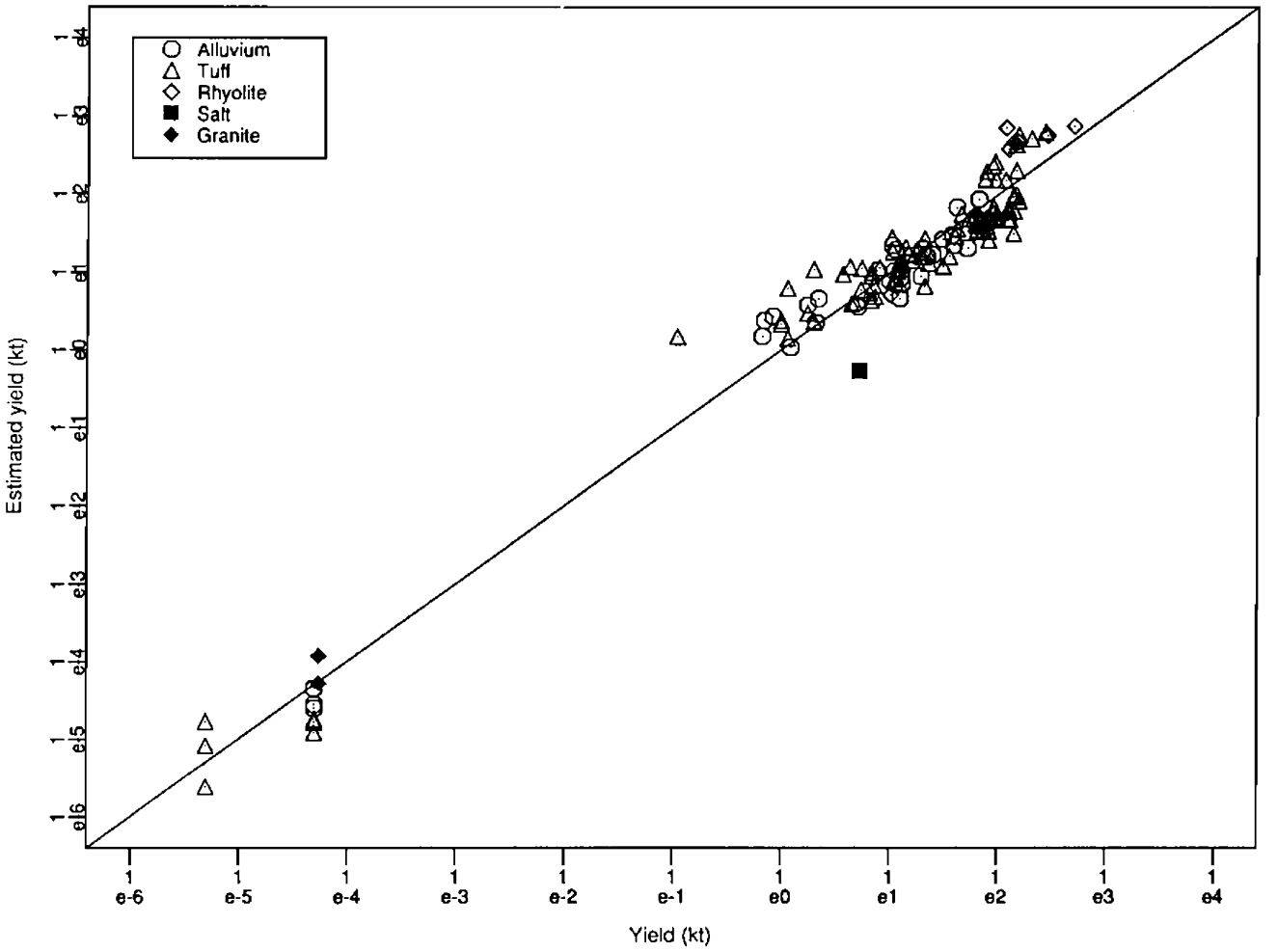

Fig. 12. Yield estimated from (43) versus actual yield by material. As with the cavity radius and moment results, the hard-rock source radii randomly overlay those for porous rocks. Also the chemical explosions ($W < 1\times10^{-4}$ kt) are seen to be consistent with the nuclear ones. The reduction of variance due to (43) over a simple source radius, yield relationship can be seen by comparing this figure with Fig. 11. The 95% confidence level F-value is 1.93 for Fig. 11 while in this figure it is 1.65.

be acquired to improve confidence. An effort should also be made to better understand how shear strength should be factored into these empirical relationships, to understand the trade-offs between shear strength and depth, and to acquire shear strength information. Some of the variance in each of the empirical relationships could, also, be due to the initial source volume as suggested by Glenn [1990] and information on it should be collected to determine its impact.

What was not found in this study was also significant. No significant differences between hard-rocks and porous ones were found beyond what is accounted for by the shear modulus and gas porosity. Nor was any evidence found that chemical explosions are significantly different from nuclear explosions, in agreement with the finite difference calculations of Killian et al. [1987]. And no differences were found in either the moment or corner frequency due to the measurement realm, near-field versus far-field. However, the hard-rock data set is very small so that the possibility may still exist that hard-rocks should be treated differently than porous ones.

The lack of significant differences between the two types of explosives suggests that experiments employing chemical explosives could be an effective means of resolving the remaining source function uncertainties. The results from chemical explosions are, in fact, very encouraging and further use should be made of such experiments to gain experience in a wider variety of materials. An experimental program designed around chemical explosions could remove many of the uncertainties and answer many questions, including the behavior of different rock types at low stresses.

Acknowledgements. Howard Patton and Paul Richards deserve special thanks for their suggestions for improving the organization and content of this paper. Janet Ricca created the database, Amanda Goldner helped out with the regression analysis and Dick Mensing helped interpret the results. The many suggestions of the reviewers were appreciated and many were incorporated. One anonymous reviewer especially prodded the authors to do a better job. This work was done under the auspices of the U.S. Department of Energy by Lawrence Livermore National Laboratory under contract W-7405-Eng-48. Funding was provided by the DOE Office of Arms Control.

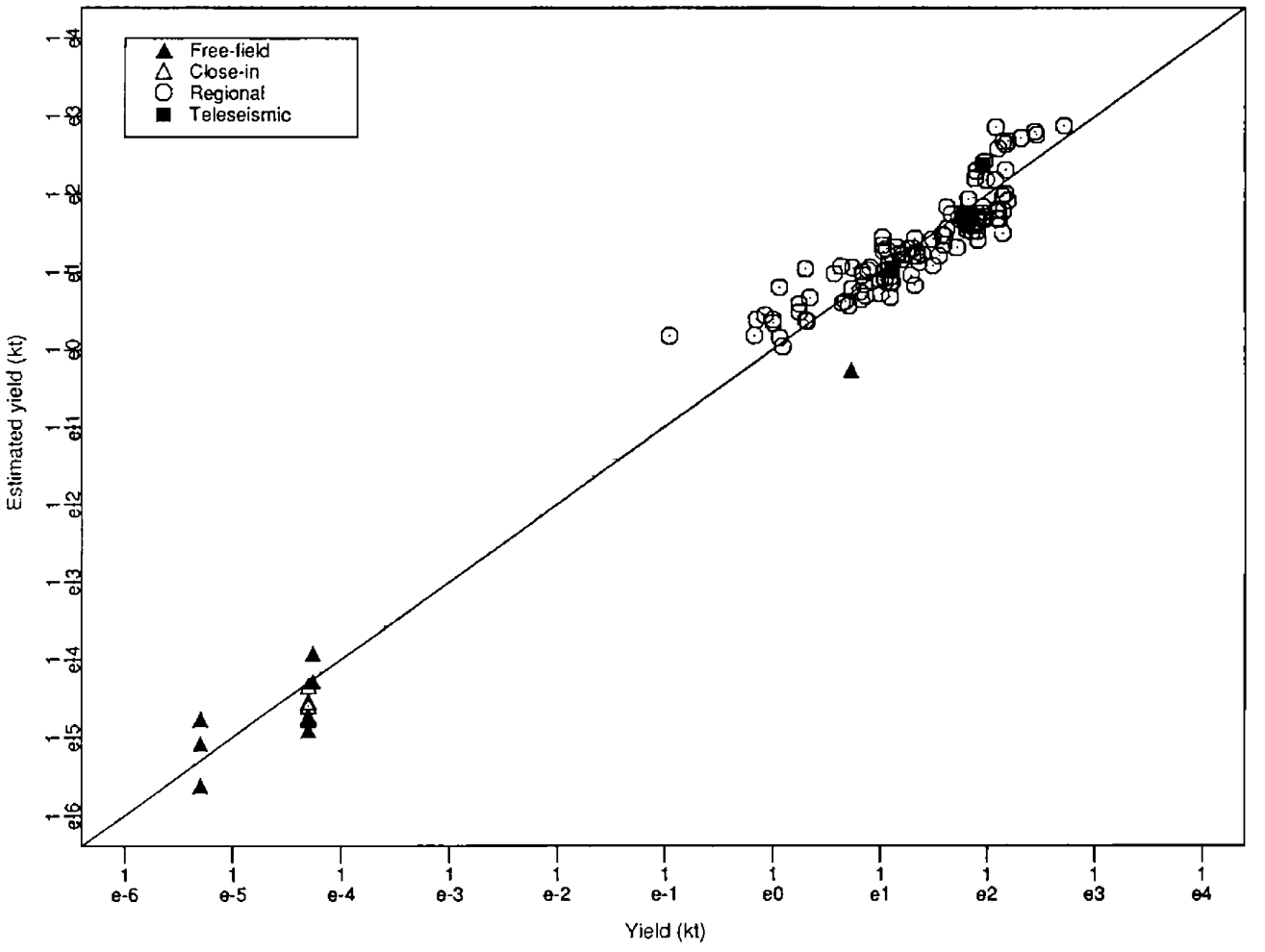

Fig. 13. Yield estimated from (43) versus actual yield by measurement regime. As with the moment data, the various regimes are randomly mixed.

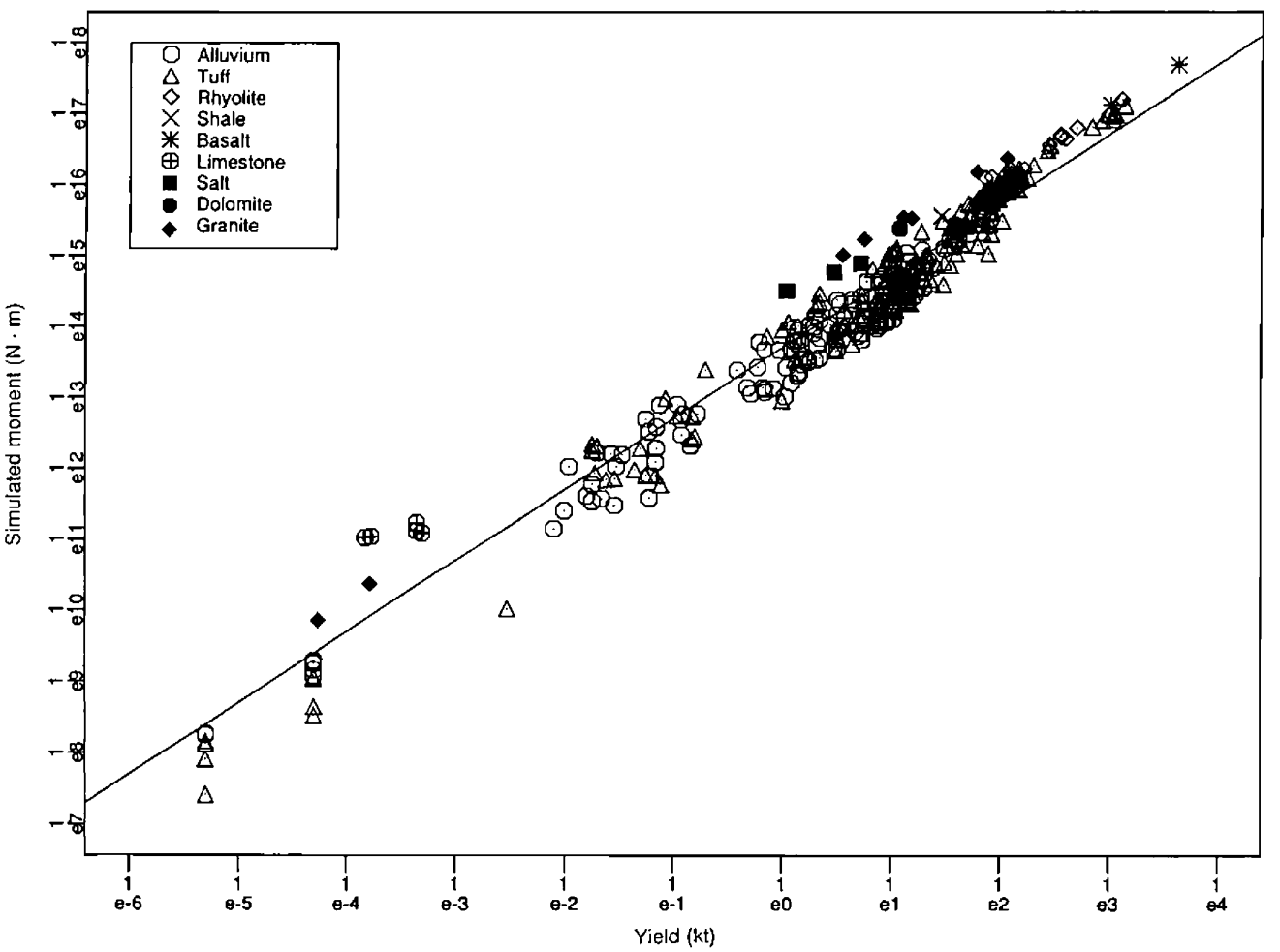

Fig. 14. Simulated seismic moment. (41) was evaluated for all the events in the database with the required material parameters. Considerable variation across NTS should be expected. It is easy to see how a small set of events could appear to have a slope different than the true slope.

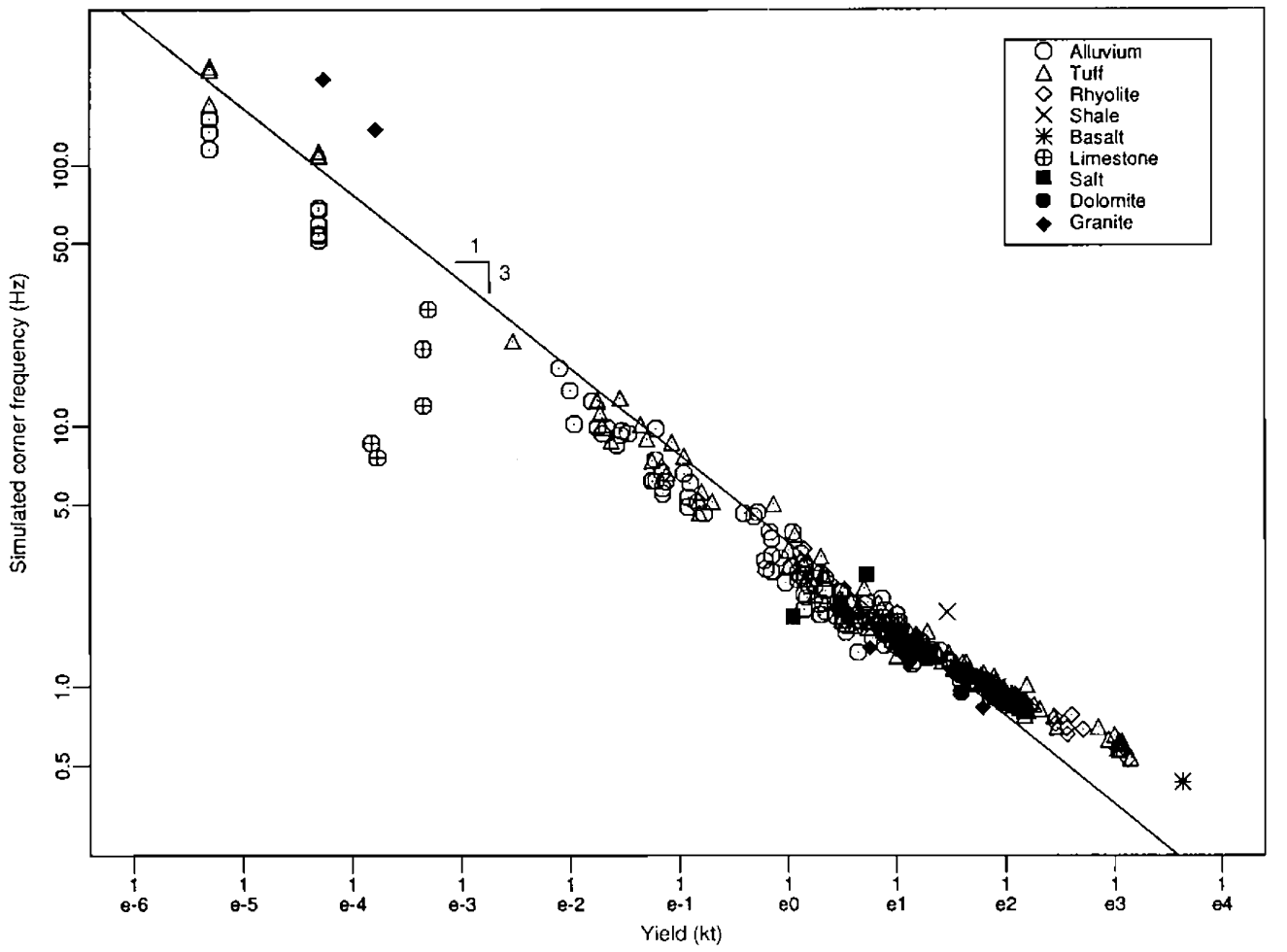

Fig. 15. Simulated corner frequency. (43) was evaluated for all the events in the database with the required material parameters. A systematic change in slope should be expected with increasing depth (yield).

References

Aki, K., M. Bouchon, and P. Reasenberg, Seismic Source Function for an Underground Nuclear Explosion, *Bull. Seism. Soc. Am.*, *64*, 131–148, 1974.

Aki, K., and P. G. Richards, *Quantitative Seismology: Theory and Methods*, Vol. 1, W. H. Freeman and Co., San Francisco, 1980.

Bache, T. C., Estimating the Yield of Underground Nuclear Explosions, *Bull. Seism. Soc. Am.*, *72*, S131–S168, 1982.

Baker, W. E., P. S. Westine, and F. T. Dodge, *Similarity Methods in Engineering Dynamics*, Hayden Book Company, Inc., Rochelle Park, NJ, p. 257, 1973.

Basham, P. W., and R. B. Horner, Seismic Magnitudes of Underground Nuclear Explosions, *Bull. Seism. Soc. Am.*, *63*, 105–131, 1973.

Bateman, H., *Tables of Integral Transforms*, Vol. I NR 043-045, McGraw-Hill Book Company, Inc., New York, 1954.

Berg, J. W., Jr., and G. E. Papageorge, Elastic Displacement of Primary Waves from Explosive Sources, *Bull. Seism. Soc. Am.*, *54*, 947–959, 1964.

Blake, F. G., Jr., Spherical Wave Propagation in Solid Media, *J. Acoust. Soc. Am.*, *24*, 211–215, 1952.

Boardman, C. R., D. D. Rabb, and R. D. McAuthor, Responses of Four Rock Mediums to Contained Nuclear Explosions, *J. Geophys. Res.*, *69*, 3457, 1964.

Bocharov, V. S., M. N. Georgievskii, V. V. Kirichenko, and A. B. Peshkov, *Estimation of the Power of Underground Nuclear Explosions, Taking Account of their Actual Seismic Efficiency* (trans. from *Atomnaya Energiya*, *65*(2), 109–114, 1988), Plenum Publishing Corp., 1989.

Brune, J., J. Nafe, and J. Oliver, A Simplified Method for the Analysis and Synthesis of Dispersed Wave Trains, *J. Geophys. Res.*, *65*, 287, 1960.

Brune, J. N., and P. W. Pomeroy, Surface Wave Radiation Patterns for Underground Nuclear Explosions and Small-Magnitude Earthquakes, *J. Geophys. Res.*, *68*, 5005, 1963.

Burdick, L. J., and D. V. Helmberger, Time Functions Appropriate for Nuclear Explosions, *Bull Seism. Soc. Am.*, *69*, 957–973, 1979.

Burdick, L. J., T. Wallace, and T. Lay, Modeling Near-Field and Teleseismic Observations from the Amchitka Test Site, *J. Geophys. Res.*, *89*, 4373–4388, 1984.

Butkovich, T. R., *Cavities Produced by Underground Nuclear Explosions*, Lawrence Livermore National Laboratory, Livermore, CA, UCRL-52097, 1976.

Cagniard, L., E. A. Flinn, and C. H. Dix, *Reflection and Refraction of Progressive Seismic Waves*, McGraw-Hill Book Company, Inc., New York, 1962.

Carpenter, E. W., R. A. Savill, and J. K. Wright, The Dependence of Seismic Signal Amplitudes on the Size of Underground Explosions, *Geophys. J.*, *6*, 426, 1962.

Chabai, A. J. On Scaling Dimensions of Craters Produced by Buried Explosives, *J. Geophys. Res.*, *70*, 5075, 1965.

Cheng, D. K. *Analysis of Linear Systems*, Addison-Wesley, Reading, MA, 1959.

Closmann, P. J. On the Prediction of Cavity Radius Produced by an Underground Nuclear Explosion, *J. Geophys. Res.*, *74*, 3935, 1969.

Crowley, B. K. *Scaling Criteria for Rock Dynamic Experiments*, Lawrence Livermore National Laboratory, Livermore, CA, UCRL-71879, 1970.

Denny, M. D., NTS Seismic Yield Experiment: An Overview, *Seism. Res. Lett.*, *61*, 11, 1990.

Denny, M. D., and D. M. Goodman, A Case Study of the Seismic Source Function: SALMON and STERLING Reevaluated, *J. Geophys. Res.*, *95*, 19,705–19,723, 1990.

Douglas, A., and J. A. Hudson, Comments on "Time Functions Appropriate for Nuclear Explosions," By L. J. Burdick and D. V. Helmberger and "Seismic Source Functions and Attenuation from Local and Teleseismic Observations of the NTS Events Jorum and Handley," By D. V. Helmberger and D. M. Handley, *Bull. Seism. Soc. Am.*, *73*, 1255–1264, 1983.

Gaskell, T. F., The Relation Between Size of Charge and Amplitude of Refracted Wave, *Geophys. Prosp.*, *IV*, 13, 1956.

Glenn, L. A., *Ab Initio Calculation of the Decoupling Factor for Explosions in Porus Media*, Lawrence Livermore National Laboratory, Livermore, CA, UCRL-JC-104751, 1990.

Glenn, L. A., *Partially Decoupled Explosion Cavities*, Lawrence Livermore National Laboratory, Livermore, CA, 1991.

Glenn, L. A., Strain Hardening in Salt—Results of the Salmon Experiment, *J. Energy Res. Tech.* (Trans. ASME), *112*, No. 2, 145–148, 1990.

Grant, F. S., and G. F. West, *Interpretation Theory in Applied Geophysics*, McGraw-Hill, New York, 1965.

Gurvich, I. I., The Theory of Spherical Radiators of Seismic Waves, *Bull. Acad. Sci. USSR*, *U.D.C.534.1:550.834*, 684, 1965.

Haskell, N. A., Analytic Approximation for the Elastic Radiation from a Contained Underground Explosion, *J. Geophys. Res.*, *72*, 2583, 1967.

Haskell, N.A., A Static Theory of the Seismic Coupling of a Contained Underground Explosion, *J. Geophys. Res.*, *66*, 2937, 1961.

Helmberger, D. V., and D. M. Hadley, Seismic Source Functions and Attenuation from Local and Teleseismic Observations of the NTS Events Jorum and Handley, *Bull. Seism. Soc. Am.*, *71*, 51–67, 1981.

Helmberger, D. V., and D. G. Harkrider, Seismic Source Descriptions of Underground Explosions and a Depth Discriminate, *Geophys. J. R. astr. Soc.*, *31*, 45–66, 1972.

Higgins, G. H., and T. R. Butkovich, *Effect of Water Content, Yield, Medium, and Depth of Burst on Cavity Radii*, Lawrence Livermore National Laboratory, Livermore, CA, UCRL-50203, 1967.

Howard, N. W, *LLNL Containment Program Nuclear Test Effects and Geologic Data Base: Glossary and Parameter Definitions*, Lawrence Livermore National Laboratory, Livermore, CA, UCID-18300, Part 1, Rev. 1, 1983.

Jeffreys, H., *Collected Papers of Sir Harold Jeffreys on Geophysics and Other Sciences, Vol. 1, Theoretical and Observational Seismology*, Gordon and Breach Science Publishers, New York, 1971.

Jeffreys, H., On the Cause of Oscillatory Movement in Seismograms, *MNGS*, *2*, 407–16, 1931.

Jeffreys, H., *The Earth Its Origin History and Physical Constitution*, Cambridge University Press, Cambridge, 1976.

Johnson, L. R., Source Characteristics of Two Underground Nuclear Explosions, *Geophys. J.*, *95*, 15–30, 1988.

Johnson, L. R., and T. V. McEvilly, *OSSY Source Characterization—Summary Report*, Lawrence Berkeley Laboratory, Berkeley, CA, LBL-29783, 1990.

Killian, B. G., J. R. Rocco, and E. J. Rinehart, *Comparisons of Nuclear-TNT Equivalencies and Effects Environments in Different Geologic Media*, Defense Nuclear Agency, Washington, DC, DNA-TR-87-152, 1987.

Larson, D. B., Explosive-Induced Wave Propagation in Nugget Sandstone, *J. Geophys. Res.*, *89*, 9415–9424, 1984.

Larson, D. B., Inelastic Wave Propagation in Sodium Chloride, *Bull. Seism. Soc. Am.*, *72*, 2107–2130, 1982.

Latter, A. L., E. A. Martinelli, and E. Teller, Seismic Scaling Law for Underground Explosions, *Phys. Flu.*, *2*, 280, 1959.

Lay, T., D. V. Helmberger, and D. G. Harkrider, Source Models and Yield-Scaling Relations for Underground Nuclear Explosions at Amchitka Island, *Bull. Seism. Soc. Am.*, *74*, 843–862, 1984.

Liebermann, R. C., and P. W. Pomeroy, Relative Excitation of Surface Waves by Earthquakes and Underground Explosions, *J. Geophys. Res.*, *74*, 1575, 1969.

Lin, W., *A Review of Soviet Studies Related to Peaceful Underground Nuclear Explosions*, Lawrence Livermore National Laboratory, Livermore, CA, UCID-17729, 1978.

Marshall, P. D., D. L. Springer, and H. C. Rodean, Magnitude Corrections for Attenuation in the Upper Mantle, *Geophys. J. R. astr. Soc.*, *57*, 609–638, 1979.

Massé, R. P., Review of Seismic Source Models for Underground Nuclear Explosions, *Bull. Seism. Soc. Am.*, *71*, 1249–1268, 1981.

McEvilly, T. V., and L. R. Johnson, *Regional Studies with Broadband Data*, Geophysical Laboratory, GL-TR-89-0224, 57 pp., 1989.

McGarr, A., and J. Bicknell, Comparison of Ground Motion from Tremors and Explosions in Deep Gold Mines, *J. Geophys. Res.*, *95*,

21,777–21,792, 1990.

Michaud, L., *Explosions nucleáires souterraines: étude des rayons de cavité*, Centre d'Etudes de Bruyères-le-Châtel, CEA-R-3594, 1968.

Molnar, P., *P*-wave Spectra from Underground Nuclear Explosions, *Geophys. J. R. astr. Soc., 23*, 273–287, 1971.

Molnar, P., J. Savino, L. R. Sykes, R. C. Liebermann, G. Hade, and P. W. Pomeroy, Small Earthquakes and Explosions in Western North America Recorded by New High Gain, Long Period Seismographs, *Nature, 224*, 1269, 1969.

Mueller, R. A., Seismic Energy Efficiency of Underground Nuclear Detonations, *Bull. Seism. Soc. Am., 59*, 2311–2323, 1969.

Mueller, R. A., and J. R. Murphy, Seismic Characteristics of Underground Nuclear Detonations Part I. Seismic Spectrum Scaling, *Bull. Seism. Soc. Am., 61*, 1675–1692, 1971.

Müller, G., Seismic Moment and Long-Period Radiation of Underground Nuclear Explosions, *Bull. Seism. Soc. Am., 63*, 847–857, 1973.

Murphy, J. R., Discussion of "Seismic Source Function for an Underground Nuclear Explosion" by Keiiti Aki, Michel Bouchon, and Paul Reasenberg, *Bull. Seism. Soc. Am., 64*, 1595–1597, 1974.

Murphy, J. R., Free-Field Seismic Observations from Underground Nuclear Explosions, this volume, 1991.

Murphy, J. R., Seismic Source Functions and Magnitude Determinations for Underground Nuclear Detonations, *Bull. Seism. Soc. Am., 67*, 135–158, 1977.

Murphy, J. R., and T. J. Bennett, *A Review of Available Free-Field Seismic Data from Underground Nuclear Explosions in Alluvium, Tuff, Dolomite, Sandstone-Shale and Interbedded Lava Flows*, Systems, Science and Software, La Jolla, CA, SSS-R-80-4216, 1979.

Nuckolls, J. H., *A Computer Calculation of Rainier*, Lawrence Livermore National Laboratory, Livermore, CA, UCRL-5675, 1959.

Nuttli, O. W., Yield Estimates of Nevada Test Site Explosions Obtained from Seismic Lg Waves, *J. Geophys. Res., 91*, 2137–2151, 1986.

O'Brien, P. N. S., The Relationship between Seismic Amplitude and Weight of Charge, *Geophys. Prosp., V*, 349–352, 1957.

O'Brien, P. N. S., Seismic Energy from Explosions, *Geophys. J., 3*, 29–44, 1960.

O'Brien, P. N. S., Some Experiments Concerning the Primary Seismic Pulse, *Geophys. Prosp., II*, 511–541, 1969.

Orphal, D. L., *The Cavity Formed by a Contained Underground Nuclear Detonation*, Environmental Research Corporation, MVO-1163-TM-15, 1970.

Patton, H. J., Application of Nuttli's Method to Estimate Yield of Nevada Test Site Explosions Recorded on Lawrence Livermore National Laboratory's Digital Seismic System, *Bull. Seism. Soc. Am.*, 1759–1772, 1988.

Patton, H. J., Measurements of Rayleigh-Wave Phase Velocities in Nevada: Implications for Explosion Sources and the Massachusetts Mountain Earthquake, *Bull. Seism. Soc. Am., 72*, 1329–1349, 1982.

Patton, H. J., Seismic Moment Estimation and the Scaling of the Explosion Source Spectrum, this volume, 1991.

Peppin, W. A., *P*-Wave Spectra of Nevada Test Site Events at Near and Very Near Distances: Implications for a Near-Regional Body Wave-Surface Wave Discriminant, *Bull. Seism. Soc. Am., 66*, 803–825, 1976.

Perret, W. R., *Free-Field and Surface Motion from a Nuclear Explosion in Alluvium: Merlin Event*, Sandia Laboratories, Albuquerque, NM, SC-RR-69-334, 1971.

Perret, W. R., and R. C. Bass, *Free-Field Ground Motion Induced by Underground Explosions*, Sandia National Laboratories, Albuquerque, NM, SAND-74-0252, 1975.

Rodean, H. C., *Inelastic Processes in Seismic Wave Generation by Underground Explosions*, Lawrence Livermore National Laboratory, Livermore, CA, UCRL-84515, 1981.

Rodean, H. C., *Nuclear-Explosion Seismology*, USAEC Technical Information Center, Oak Ridge, TN, 1971.

Savino, J., L. R. Sykes, R. C. Liebermann, and P. Molnar, Excitation of Seismic Surface Waves with Periods of 15 to 70 Seconds for Earthquakes and Underground Explosions, *J. Geophys. Res., 76*, 8003, 1971.

Schock, R. N., Correlation Between Rock Strength and Acoustic Velocity, *Proc. of the Monterey Containment Symposium, Montery, CA, Aug. 26–28, 1981*, Los Alamos National Laboratory, Los Alamos, NM, LA-9211-C, Vol. 1, 1981.

Sharpe, J. A., The Production of Elastic Waves by Explosion Pressures. I. Theory and Empirical Field Observations, *Geophys., 7*, 144, 1942.

Springer, D. L., and W. J. Hannon, Amplitude-Yield Scaling for Underground Nuclear Explosions, *Bull. Seism. Soc. Am., 63*, 447–500, 1973.

Stevens, J. L., Estimation of Scalar Moments from Explosion-Generated Surface Waves, *Bull. Seism. Soc. Am., 76*, 123–151, 1986.

Taylor, S. R., and G. E. Randall, The Effects of Spall on Regional Seismograms, *Geophys. Res. Lett., 16*, 211–214, 1989.

Terhune, R. W., and H. D. Glenn, *Estimate of Earth Media Shear Strength at the Nevada Test Site*, Lawrence Livermore National Laboratory, Livermore, CA, UCRL-52358, 1977.

Toksoz, M. N., A. Ben-Menahem, and D. G. Harkrider, Determination of Source Parameters of Explosions and Earthquakes by Amplitude Equalization of Seismic Surface Waves, *J. Geophys. Res., 68*, 4355, 1964.

Tsai, Yi-Ben, and K. Aki, Amplitude Spectra of Surface Waves from Small Earthquakes and Underground Nuclear Explosions, *J. Geophys. Res., 76*, 3940, 1971.

Vergino, E. S., Soviet Test Yields, *EOS, 70*, 1511, 1989.

Vergino, E. S., M. D. Denny, and S. R. Taylor, A New Look at the Explosion Source Function, *Seism. Res. Lett., 59*, 44, 1988.

Vergino, E. S., and R. W. Mensing, Yield Estimation Using Regional m_{bP_n}, *Bull. Seism. Soc. Am, 80*, 656–674, 1990.

von Seggern, D., and R. Blandford, Source Time Functions and Spectra for Underground Nuclear Explosions, *Geophys. J. R. astr. Soc., 31*, 83–97, 1972.

von Seggern, D., and D. G. Lambert, Theoretical and Observed Rayleigh-Wave Spectra for Explosions and Earthquakes, *J. Geophys. Res., 75*, 7382, 1970.

Werth, G. C., and R. F. Herbst, Comparison of Amplitudes of Seismic Waves from Nuclear Explosions in Four Mediums, *J. Geophys. Res., 68*, 1463, 1963.

Werth, G. C., R. F. Herbst, and D. L. Springer, Amplitudes of Seismic Arrivals from the M Discontinuity, *J. Geophys. Res., 67*, 1587, 1962.

Wyss, M., T. C. Hanks, and R. C. Liebermann, Comparison of *P*-Wave Spectra of Underground Explosions and Earthquakes, *J. Geophys. Res., 76*, 2716, 1971.